NASA TN D-1247

NASA TN D-1247

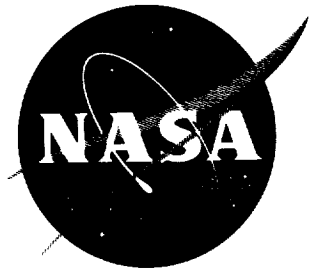

TECHNICAL NOTE

D-1247

A MATRIX METHOD FOR THE DETERMINATION OF THE NATURAL VIBRATIONS OF FREE-FREE UNSYMMETRICAL BEAMS WITH APPLICATION TO LAUNCH VEHICLES

By Vernon L. Alley, Jr., and A. Harper Gerringer

Langley Research Center
Langley Station, Hampton, Va.

NATIONAL AERONAUTICS AND SPACE ADMINISTRATION

WASHINGTON April 1962

NATIONAL AERONAUTICS AND SPACE ADMINISTRATION

TECHNICAL NOTE D-1247

A MATRIX METHOD FOR THE DETERMINATION OF THE NATURAL VIBRATIONS OF FREE-FREE UNSYMMETRICAL BEAMS WITH APPLICATION TO LAUNCH VEHICLES

By Vernon L. Alley, Jr., and A. Harper Gerringer

SUMMARY

The equations for determining the undamped natural vibrations of free-free unsymmetrical beams and launch-vehicle structures are developed herein. The analysis treats a continuous free-free system as an equivalent discrete-mass system of a finite number of degrees of freedom. The flexure-load relationships are equated by influence coefficients which are derived in the present paper by considering both flexure and deflections from local rotations. Matrix notations are used throughout the paper because of their suitability to the analysis of discrete-mass systems. Equations are developed for the dynamic equilibrium of the system, the natural frequencies and mode shapes and their first derivatives, the bending moments associated with the modes, and the influence coefficients. The results of an investigation on the accuracy of the natural frequencies and mode shapes in terms of the number of discrete masses employed in the solution are also included. The procedures are illustrated by a numerical analysis of a uniform beam, and the application of the matrix procedure to a typical launch vehicle is given.

INTRODUCTION

The undamped free-free natural modes of a structure have a wide variety of uses in engineering problems. The orthogonal properties of the mode shapes make them desirable functions for use in series solutions involving generalized coordinates, widely known as "modal form solutions." A knowledge of the time history of the natural frequencies of a spin-stabilized rocket vehicle is essential to the design of the spin program and is of value in establishing proper instrumentation for monitoring environmental responses. Modal information is also essential to proper positioning of guidance sensing devices and for investigating the stability characteristics of vehicles with closed-loop control systems.

The transient mass and structural characteristics of a typical multistage rocket vehicle require that the natural-vibration characteristics of the vehicle be known at least for the ignition and burnout times of each stage of flight and frequently for other conditions such as those at a Mach number of 1, maximum dynamic pressure, and minimum lift. For transient wind-response studies considering variable coefficients in the equations of motion, it is frequently required that the natural modes and their related properties be defined as often as 10 times during first-stage burning. These stringent requirements involve substantial engineering effort and justify the development of computing techniques adaptable to automatic digital computers.

Considerable work has been done on the problem of computing natural vibrations of beams, and a wide variety of methods are available for accomplishing such ends. However, none of the published procedures adequately and conveniently satisfy the need for volume production of modal data for launch-vehicle structures.

It is the purpose of this paper to present a solution of the natural vibrations of structures which satisfies the specific needs of the rocket vehicle designer. The procedure consists of a matrix formulation generally similar to the numerical process outlined in reference 1. The use of matrices permits the coordination of a set of computational stages to produce a single matrix equation from which the frequencies and mode shapes of the system can be obtained by application of elementary principles of matrix algebra.

The growing importance of aeroelastic behavior and the use of attitude and attitude rate sensing devices in vehicles with control systems have given rise to the need for the slopes of the natural mode shapes. The addition of the moments of the modes with proper consideration of their relative magnitudes often provides a convenient way for obtaining the composite bending moments of a structure. Consequently, the equations for the mode slopes and moments associated with the various mode shapes are also developed and presented herein.

The effects of shear deformation and rotary inertia are sometimes significant in the higher modes of oscillation, but the added complications and additional parameters necessary to incorporate these secondary influences are seldom justified and consequently these effects are not included. The engineer nevertheless should be cognizant of the potential significance of such omissions in the special cases requiring extreme accuracy of mode data.

In order to assist the user in selecting the number of masses required to yield results to a desired accuracy, data are furnished on the influence of the number of discrete masses on the accuracy of the frequencies and mode shapes of a uniform beam. In order to illustrate

the matrix operations, a detailed numerical example is furnished for a uniform beam. For the engineer unacquainted with matrix notations and methods, the elementary concepts essential to the derivations of this report are available in a number of texts on matrices such as references 2 and 3.

An application of the method to a typical rocket vehicle is presented to illustrate the input data and to show the typical output.

SYMBOLS

A	matrix of equation (10), in./lb
a	coordinate in least-error analysis, in.
a_i	scaling constant given by equation (18), in.
b	coordinate in least-error analysis, radians
c_u	coordinate to joint u, in.
D(s)	sweeping matrix given in equation (19)
E	modulus of elasticity, lb/in.^{2}
F_r	inertia force of rth mass at rth station, lb
f	natural frequency of the free-free oscillation, cps
$h_r(s)$	trial column matrix for iterating for the sth mode, in.
I	moment of inertia of structural cross-sectional area, in.^{4}
J	mass moment of inertia about the zero station, lb-in-sec^2
j_r	the jth value at the reference station r
L	total length of beam, in.
M	moment of the mass about the zero station, lb-sec^2
M_s	bending moment at the sth station, in-lb

M_o end moment in influence coefficient derivations, in-lb

m total mass of system $= \sum_{n=0}^{p-1} m_n$, lb-sec^2/in.

m_n nth discrete mass, lb-sec^2/in.

P force in influence-coefficient derivation, lb

p number of discrete masses in the system

q_i reference mode deflection at x_i for comparative purposes by least-square method, in.

$\bar{r}$ radius of gyration of the total mass about the center of gravity, in.

U strain energy, in-lb

V_o boundary shear force in influence-coefficient derivation, lb

v number of joints considered in the structure

$v_i = x_i + \frac{L}{2p}$ coordinate from left end of uniform beam, in.

X moment matrix, in.

x coordinate along the length of the vehicle, in.

x_r coordinate to the rth station, in.

$\bar{x}$ distance to the center of gravity from the 0th mass, in.

Y general function of x, units vary

$Y_r(s)$ an approximation to the sth mode shape, in.

$y_n(s)$ deflection at x_n of the sth natural mode, in.

δy_i discrepancy between modes at the ith point determined by the matrix methods and by exact method

$\alpha_{r,n}$ deflection influence coefficient for elastic bending only, deflection at $x = x_r$ due to a unit load at $x = x_n$ when cantilevered at $x = 0$, in./lb

$\beta_r = \int_0^{x_r} \frac{x^2}{EI}\,dx$, in./lb

γ rotation at a joint due to a load P_n at x_n, radians

$\delta_{r,n}^{(u)}$ deflection influence coefficient considering elastic rotation of joint u only, deflection at $x = x_r$ due to a unit load at $x = x_n$ when cantilevered at $x = 0$, in./lb

ϵ_f error in natural frequencies between matrix method and comparative exact solution, percent

ϵ_y error in mode shapes between matrix method and comparative exact solution, percent.

$\zeta(x_i)$ mode displacements of comparative exact solution

$\zeta_{r,n}^{(u)}$ slope influence coefficient considering elastic rotation of joint u only; the slope at $x = x_r$ due to a unit load at $x = x_n$, when cantilevered at $x = 0$, radians/lb

$\eta_r = \int_0^{x_r} \frac{1}{EI}\,dx$, $lb^{-1}\text{-in.}^{-1}$

θ_r slope at the rth station, radians

$\theta_{r,n}$ slope at $x = x_r$ due to a load P at $x = x_n$ when cantilevered at $x = 0$, considering beam flexure only, radians

$\nu_{r,n}$ slope influence coefficient considering beam flexure only, slope at $x = x_r$ due to a unit load at $x = x_n$ when cantilevered at $x = 0$, radians/lb

κ_u joint rotation constant for joint u, radians/in-lb

λ_s sth eigenvalue of equation (10) or equation (20), $1/\omega_s^2 m$, $\text{in.}/\text{lb-radians}^2$

$$\mu_r = \int_0^{x_r} \frac{x}{EI}\, dx, \ lb^{-1}$$

$\rho_{r,n}$ total slope influence coefficient considering both bending and joint effects; the slope at $x = x_r$ due to a unit load at $x = x_n$ when cantilevered at $x = 0$, radians/lb

$\sigma_{r,n}$ total deflection influence coefficient considering both bending and joint effects, the deflection at $x = x_r$ due to a unit load at $x = x_n$ when cantilevered at $x = 0$, in./lb

ω circular frequency for natural vibrations of the free-free system, radians/sec

$\{\}, [\ ], [\,], [\,], [1], \{\}^T$ column, diagonal, square, row, unit, and transpose matrices, respectively

Subscripts:

i,j,n,r,s,u integers

DERIVATION OF THE EQUATIONS OF MOTION

The derivation of the equations of motion for the free-free structure including detail developments for determining boundary values, mode slopes, mode moments, and all necessary influence coefficients is given in this section.

General Procedure for a Free-Free Unsymmetrical System

The solution requires that an equivalent system of discrete masses, such as that illustrated in the following sketch, be devised that will adequately represent the continuous system. The load-deflection characteristics are stated by use of cantilever influence coefficients which are derived by use of elementary beam-flexural theory for small displacements and with appropriate consideration of local joint rotations. Second-order effects such as shear deformation and rotary inertia are not included.

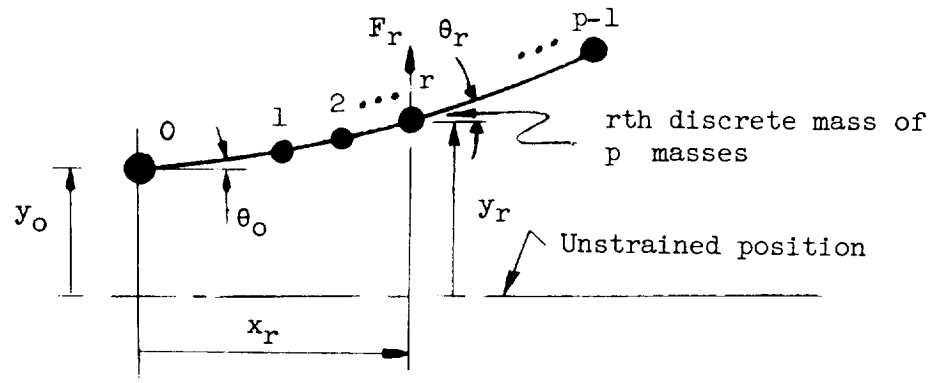

Sketch 1

Let $\sigma_{r,n}$ define the deflection at $x = x_r$ due to a unit load at $x = x_n$ when cantilevered at $x = 0$. Then the deflection at x_r for a system of p discrete masses can be stated.

$$y_r = \sum_{n=1}^{p-1} F_n \sigma_{r,n} + \theta_o x_r + y_o \tag{1}$$

For a free-free vibration, the forces F_n are composed only of the inertial loads which according to the laws of conservation of linear and angular momentum satisfy the equations

$$\sum_{n=0}^{p-1} F_n = 0 \tag{2}$$

$$\sum_{n=0}^{p-1} F_n x_n = 0 \tag{3}$$

For steady-state harmonic oscillations at frequency ω

$$F_n = m_n \omega^2 y_n \tag{4}$$

The substitution of equation (4) into equations (1), (2), and (3) yields $p + 1$ equations for $p + 1$ unknowns

$$y_r = \omega^2 \sum_{n=1}^{p-1} \sigma_{r,n} m_n y_n + \theta_o x_r + y_o \tag{5a}$$

$$m_o y_o + \sum_{n=1}^{p-1} m_n y_n = 0 \tag{5b}$$

$$\sum_{n=1}^{p-1} x_n m_n y_n = 0 \tag{5c}$$

By changing the n subscripts to r in equations (5b) and (5c), substituting equation (5a) into the modified equations in place of y_r, and introducing the following notations:

$$m_o + \sum_{r=1}^{p-1} m_r = m$$

which is the total mass of the system,

$$\sum_{r=1}^{p-1} m_r x_r = M$$

which is the moment of the mass about the zero station, and

$$\sum_{r=1}^{p-1} m_r x_r^2 = J$$

which is the mass moment of inertia about the zero station and since $\sigma_{o,n} = 0$ by definition, then equations (5b) and (5c) become in matrix form

$$\theta_o M + m y_o + \omega^2 \left[1\right]\left[m_r\right]\left[\sigma_{r,n}\right]\left[m_n\right]\left\{y_n\right\} = 0 \tag{6}$$

and

$$\theta_o J + M y_o + \omega^2 \left[x_r\right]\left[m_r\right]\left[\sigma_{r,n}\right]\left[m_n\right]\left\{y_n\right\} = 0 \tag{7}$$

$$\begin{pmatrix} n = 1, 2, 3 \ldots p-1 \\ r = 1, 2, 3 \ldots p-1 \end{pmatrix}$$

Noting that

$$M = m\bar{x}$$

$$J = m\left(\bar{r}^2 + \bar{x}^2\right)$$

where: $\bar{x}$ is the distance to the center of gravity of the system from the x origin, and
$\bar{r}$ is the radius of gyration of the total mass about the center of gravity of the system

L 1 9 3 3 then with these notations and by solving equations (6) and (7) simultaneously for θ_o and y_o, it is found that

$$\theta_o = \frac{\omega^2 m}{\bar{x}} \frac{\bar{x}^2}{\bar{r}^2}\left[1 - \frac{x_r}{\bar{x}}\right]\left[\frac{m_r}{m}\right]\left[\sigma_{r,n}\right]\left[\frac{m_n}{m}\right]\left\{y_n\right\} \tag{8}$$

$$y_o = -\omega^2 m\left[1 + \frac{\bar{x}^2}{\bar{r}^2} - \frac{\bar{x}^2}{\bar{r}^2}\frac{x_r}{\bar{x}}\right]\left[\frac{m_r}{m}\right]\left[\sigma_{r,n}\right]\left[\frac{m_n}{m}\right]\left\{y_n\right\} \tag{9}$$

By substituting equations (8) and (9) into equation (5a) and making some permissible interchanges in subscripts, the desired form of the equations of motion in matrix notation is obtained as

$$\frac{1}{\omega^2 m}\left\{y_r\right\} = \left[\left[1\right] + \left[\frac{\bar{x}^2}{\bar{r}^2}\left\{\frac{x_r}{\bar{x}}\right\}\left[1 - \frac{x_r}{\bar{x}}\right] - \left\{1\right\}\left[1 + \frac{\bar{x}^2}{\bar{r}^2} - \frac{\bar{x}^2}{\bar{r}^2}\frac{x_r}{\bar{x}}\right]\left[\frac{m_r}{m}\right]\right]\left[\sigma_{r,n}\right]\left[\frac{m_r}{m}\right]\left\{y_r\right\}$$

$$\begin{pmatrix} n = 1, 2, 3 \ldots p-1 \\ r = 1, 2, 3 \ldots p-1 \end{pmatrix} \tag{10}$$

The solution of equation (10), which is of the familiar form of an eigenvalue problem, that is;

$$\lambda_s\left\{y_r(s)\right\} = \left[A\right]\left\{y_r(s)\right\} \tag{10a}$$

will yield the natural frequencies and natural mode shapes of the dynamic system. The bracketed letter (s) added to the modal column y_r is henceforth used as needed to designate the particular solution of the $p - 1$ possible solutions of equation (10).

The basic matrices necessary for generating the A matrix of equation (10a) are $\left\{\frac{x_r}{\bar{x}}\right\}$, $\left[\frac{m_r}{m}\right]$, and $\left[\sigma_{r,n}\right]$. The first two of these matrices as well as the necessary parameters, $\bar{x}$ and $\bar{r}$, are computed readily once the magnitudes and locations of the discrete masses are established. The major work in the generation of equation (10) lies in developing the $\sigma_{r,n}$ matrix for which detailed considerations are submitted subsequently.

Boundary Values, y_o and θ_o

The number of unknown deflections in equation (10) is $p - 1$, one less than the number of masses comprising the discrete mass system. This reduction in order, highly desirable when the modes are computed manually, is a direct result of choosing the origin of the x coordinate at the end mass. However, by virtue of this choice, the y_o value is lost from the modal column and must be determined separately. The value of y_o could be determined from the explicit expression given by equation (9), but a simpler solution comes from the equilibrium condition of equation (5b), which is

$$m_o y_o(s) + \sum_{n=1}^{p-1} m_n y_n(s) = 0$$

Solving for $y_o(s)$ and interchanging the subscripts gives

$$y_o(s) = -\frac{1}{m_o/m}\left[1\right]\left[\frac{m_r}{m}\right]\left\{y_r(s)\right\} \qquad (11)$$

The boundary slope θ_o is given by equation (8). Equations (8) and (11) are the expressions for the boundary values of the problem. The $\left\{y_r\right\}$ column used in both equations is obtained from the solution of equation (10).

A Method for Solution of Equation (10)

It is evident from an inspection of equation (10) that the A matrix of equation (10a) is not a symmetrical matrix, and therefore the method of solution must be one appropriate to unsymmetrical matrices. Also,

since the modal column y_r contains only the elements from $r = 1$ to $p - 1$ and excludes y_o, the conventional orthogonality relationship of the eigenvectors does not apply, that is, for equation (10)

$$\left[y_r(s)\right]\left[\frac{m_r}{m}\right]\left\{y_r(j)\right\} \neq 0 \qquad \begin{pmatrix} s = 1, 2, 3 \ldots p - 1 \\ j = 1, 2, 3 \ldots p - 1 \end{pmatrix}$$

Since these particular characteristics of equation (10) preclude solutions for the nondominant eigenvalues by many of the conventional procedures, a detailed explanation follows for the general solution of the specific problem for both the dominant and nondominant eigenvalues and eigenvectors. A special orthogonality relationship applicable to equation (10) is necessary to the solution and must first be developed.

Special orthogonality relationship.- Multiplying equation (8) by $\lambda_i\{x_r\}$ and equation (9) by $\lambda_i\{1\}$ and subtracting the two results from equation (10) yields

$$\lambda_i\left\{\left\{y_r(i)\right\} - y_o(i)\{1\} - \theta_o(i)\left\{x_r\right\}\right\} = \left[\sigma_{r,n}\right]\left[\frac{m_r}{m}\right]\left\{y_r(i)\right\} \tag{12}$$

Premultiplying this result by $\left[y_r(j)\right]\left[\frac{m_r}{m}\right]$ and noting that from equation (5c)

$$\left[y_r\right]\left[\frac{m_r}{m}\right]\left\{x_r\right\} = 0$$

gives

$$\lambda_i\left[y_r(j)\right]\left[\frac{m_r}{m}\right]\left\{y_r(i) - y_o(i)\right\} = \left[y_r(j)\right]\left[\frac{m_r}{m}\right]\left[\sigma_{r,n}\right]\left[\frac{m_r}{m}\right]\left\{y_r(i)\right\} \tag{12a}$$

By expressing equation (12) in terms of the jth mode instead of the ith, premultiplying that expression by $\left[y_r(i)\right]\left[\frac{m_r}{m}\right]$, and using the preceding condition from equation (5c), it follows that

$$\lambda_j\left[y_r(i)\right]\left[\frac{m_r}{m}\right]\left\{y_r(j) - y_o(j)\right\} = \left[y_r(i)\right]\left[\frac{m_r}{m}\right]\left[\sigma_{r,n}\right]\left[\frac{m_r}{m}\right]\left\{y_r(j)\right\} \tag{13}$$

From equation (11),

$$y_o(i) = - \frac{m}{m_o}\left[1\right]\left[\frac{m_r}{m}\right]\left\{y_r(i)\right\}$$

and

$$y_o(j) = - \frac{m}{m_o}\left[1\right]\left[\frac{m_r}{m}\right]\left\{y_r(j)\right\}$$

and because of the symmetry of $\left[\frac{m_r}{m}\right]$ and $\left[\sigma_{r,n}\right]$

$$\left[y_r(j)\right]\left[\frac{m_r}{m}\right]\left\{1\right\} = \left[1\right]\left[\frac{m_r}{m}\right]\left\{y_r(j)\right\}$$

$$\left[y_r(i)\right]\left[\frac{m_r}{m}\right]\left\{1\right\} = \left[1\right]\left[\frac{m_r}{m}\right]\left\{y_r(i)\right\}$$

and

$$\left[y_r(i)\right]\left[\frac{m_r}{m}\right]\left[\sigma_{r,n}\right]\left[\frac{m_r}{m}\right]\left\{y_r(j)\right\} = \left[y_r(j)\right]\left[\frac{m_r}{m}\right]\left[\sigma_{r,n}\right]\left[\frac{m_r}{m}\right]\left\{y_r(i)\right\}$$

Subtracting equation (13) from (12a) and utilizing the preceding relationships yields

$$\left(\lambda_i - \lambda_j\right)\left[y_r(j) - y_o(j)\right]\left[\frac{m_r}{m}\right]\left\{y_r(i)\right\} = 0 \qquad (14)$$

from which it is established when $j \neq i$ that

$$\left[y_r(j) - y_o(j)\right]\left[\frac{m_r}{m}\right]\left[y_r(i)\right] = 0 \qquad (j \neq i) \qquad (14a)$$

Equation (14a) is the special orthogonality relationship appropriate to the solutions of equation (10).

Iteration solution of equation (10).- A recurrence equation is developed for an iterative solution of equation (10) that will converge to the desired eigenvalue and eigenvector.

In the solution for the eigenvalues and eigenvectors of equation (10) there will be $p - 1$ linearly independent eigenvectors of which $p - 2$ are the flexible mode shapes and one, associated with a zero eigenvalue, has no physical significance. In the specific application, if repeated eigenvalues exist they nevertheless will not possess identical eigenvectors. The eigenvector associated with the zero eigenvalue is distinct and can be shown to be

$$\left\{y_r\right\}_{\lambda=0} = \left[\frac{m_r}{m}\right]^{-1}\left[\sigma_{r,n}\right]^{-1}\left\{\frac{x_r}{\bar{x}}\right\}$$

Let an approximation $\left\{Y_r(s)\right\}$ to the sth mode be a linear combination of the actual $(p - 1)$ linearly independent eigenvectors of the matrix A; that is,

$$\left\{Y_r(s)\right\} = a_1\left\{y_r(1)\right\} + a_2\left\{y_r(2)\right\} + \ldots + a_{p-1}\left\{y_r(p-1)\right\} \qquad (15)$$

where $\left\{y_r(1)\right\}, \left\{y_r(2)\right\}, \ldots \left\{y_r(p-1)\right\}$ are normalized eigenvectors arranged in a sequence of decreasing magnitude of their eigenvalues, that is, $\lambda_1 > \lambda_2 > \lambda_3 \ldots \lambda_{p-2} > \lambda_{p-1}$ and $\lambda_{p-1} = 0$, and $a_1, a_2, \ldots a_{p-1}$ are the scaling constants for their respective modes.

Assume that $\left\{y_r(1)\right\}$ to $\left\{y_r(s-1)\right\}$ and their proportionality constants $a_1, a_2, \ldots a_{s-1}$ have been previously determined. Subtracting the products of known eigenvectors and their scaling constants from the approximation $\left\{Y_r(s)\right\}$ to the sth mode gives the following function $\left\{h_r(s)\right\}$ that is free of the components of the first $s - 1$ modes:

$$\begin{aligned}\left\{h_r(s)\right\} &= \left\{Y_r(s)\right\} - a_1\left\{y_r(1)\right\} - a_2\left\{y_r(2)\right\} - \ldots - a_{s-1}\left\{y_r(s-1)\right\} \\ &= a_s\left\{y_r(s)\right\} + a_{s+1}\left\{y_r(s+1)\right\} + \ldots + a_{p-1}\left\{y_r(p-1)\right\} \qquad (16)\end{aligned}$$

Premultiplying (16) by the A matrix of equation (10a) and recalling from equation (10a) that $\left[A\right]\left\{y_r(s)\right\} = \lambda_s\left\{y_r(s)\right\}$, then

$$\left[A\right]\left\{h_r(s)\right\} = a_s\lambda_s\left\{y_r(s)\right\} + a_{s+1}\lambda_{s+1}\left\{y_r(s+1)\right\} + \ldots + a_{p-1}\lambda_{p-1}\left\{y_r(p-1)\right\} \tag{17}$$

Repeated premultiplication by the A matrix m times results in

$$\left[A\right]^m\left\{h_r(s)\right\} = a_s\lambda_s{}^m\left\{y_r(s)\right\} + a_{s+1}\lambda_{s+1}{}^m\left\{y(s+1)\right\} + \ldots + a_{p-1}\lambda_{p-1}{}^m\left\{y_r(p-1)\right\} \tag{17a}$$

Since $\lambda_s > \lambda_{s+1} > \ldots > \lambda_{p-1}$ and if the process is continued sufficiently, a_s times the mth power of λ_s will predominate over all other terms on the right-hand side of equation (17a). By continuing the premultiplication by the A matrix until the sum of the $s+1$ to the $p-1$ terms becomes insignificant in comparison with the s term, then it can be stated that

$$\left[A\right]^m\left\{h_r(s)\right\} = a_s\lambda_s{}^m\left\{y_r(s)\right\} \tag{17b}$$

It is thus proven that by repeated premultiplication by $\left[A\right]$ of an assumed function of the characteristics of $\left\{h_r(s)\right\}$, the process will converge on the modal column $y_r(s)$ times a scalar $a_s\lambda_s{}^m$. Normalizing the results of (17b) by dividing by $a_s\lambda_s{}^m$ and using the normalized column as a final trial eigenvector results in the desired solution

$$\left[A\right]\left\{y_r(s)\right\} = \lambda_s\left\{y_r(s)\right\}$$

The scalar quantity $a_s\lambda_s{}^m$ resulting from m repeated premultiplication of $\left\{h_r(s)\right\}$ by $\left[A\right]$ is generally an enormously large number and leads to cumbersome numerical operations. This problem can be alleviated by frequent normalizing of the $a_s\lambda_s{}^m\left\{y_r(s)\right\}$ column as needed

since it does not alter the convergence of the process. The preceding proof of convergence to the dominant eigenvector is similar to the procedure used in reference 4.

The function $\left\{h_r(s)\right\}$ of equation (16), shown previously to converge on $\left\{y_r(s)\right\}$, must now be developed in detail. The column, $\left\{Y_r(s)\right\}$ in the function $\left\{h_r(s)\right\}$, is an estimated expression for the sth mode and may be chosen quite arbitrarily, yet a good estimation is advantageous since it will greatly increase the rate of convergence of the iteration process. The eigenvectors $\left\{y_r(1)\right\}$, $\left\{y_r(2)\right\}$, . . . $\left\{y_r(s-1)\right\}$ must have been determined before $\left\{h_r(s)\right\}$ can be evaluated. The a_1, a_2, . . . a_{s-1} coefficients remain to be determined which can be done by use of the special orthogonality condition of equation (14a).

By multiplying equation (15) by $\left[y_r(i) - y_o(i)\right]\left[\frac{m_r}{m}\right]$ and observing the orthogonality relationship of equation (14a), it is found that

$$a_i = \frac{\left[y_r(i) - y_o(i)\right]\left[\frac{m_r}{m}\right]\left\{Y_r(s)\right\}}{\left[y_r(i) - y_o(i)\right]\left[\frac{m_r}{m}\right]\left\{y_r(i)\right\}} \tag{18}$$

Substituting expressions of the type of equation (18) into the equations for $\left\{h_r(s)\right\}$, equation (16), for values of i from 1 to s - 1 yields

$$\left\{h_r(s)\right\} = \left[\left[1\right] - \frac{\left\{y_r(1)\right\}\left[y_r(1) - y_o(1)\right]\left[\frac{m_r}{m}\right]}{\left[y_r(1) - y_o(1)\right]\left[\frac{m_r}{m}\right]\left\{y_r(1)\right\}} - \frac{\left\{y_r(2)\right\}\left[y_r(2) - y_o(2)\right]\left[\frac{m_r}{m}\right]}{\left[y_r(2) - y_o(2)\right]\left[\frac{m_r}{m}\right]\left\{y_r(2)\right\}} - \ldots \right.$$

$$\left. - \frac{\left\{y_r(s-1)\right\}\left[y_r(s-1) - y_o(s-1)\right]\left[\frac{m_r}{m}\right]}{\left[y_r(s-1) - y_o(s-1)\right]\left[\frac{m_r}{m}\right]\left\{y_r(s-1)\right\}}\right]\left\{Y_r(s)\right\}$$

$$= \left[D(s)\right]\left\{Y_r(s)\right\} \tag{19}$$

Premultiplying equation (19) by the $[A]$ matrix results in a supplementary equation to (10a) that will converge upon the nondominant sth eigenvector upon repeated premultiplication by the product $[A][D(s)]$, thus

$$\lambda_s\{y_r(s)\} = [A][D(s)]\{y_r(s)\} \qquad \begin{pmatrix} r = 1, 2, 3 \ldots p - 1 \\ y_r(s = 0) = 0 \end{pmatrix} \tag{20}$$

where $[D(s)]$ is the square matrix of equation (19) and is a special sweeping matrix. Equation (20) for $s = 1$ degenerates to equation (10a), and consequently it can be seen that equation (20) is a general expression from which both dominant and nondominant solutions for the natural modes and frequencies can be obtained.

L 1933

Mode Slopes

Let $\rho_{r,n}$ be the slope at $x = x_r$ due to a unit load at $x = x_n$ when cantilevered at $x = 0$, then, the total slope θ_r at the rth station can be expressed as

$$\{\theta_r\} = \theta_o\{1\} + [\rho_{r,n}]\{F_r\}$$

Substituting equation (8) for θ_o and equation (4) for F_r yields

$$\{\theta_r\} = m\omega^2\left[\frac{\bar{x}}{\bar{r}^2}\{1\}\left[1 - \frac{x_r}{\bar{x}}\right]\left[\frac{m_r}{m}\right][\sigma_{r,n}] + [\rho_{r,n}]\right]\left[\frac{m_r}{m}\right]\{y_r\} \tag{21}$$

which relates the desired slopes explicitly to the modal column of equation (10).

Mode Moments

By letting M_s equal the bending moment at the sth station of a natural mode, then

$$M_s = \sum_{r=0}^{s} F_r(x_s - x_r) = F_o x_s + \sum_{r=1}^{s} F_r(x_s - x_r)$$

Substituting equation (4) for F_r and equation (11) for y_o and expressing in matrix form gives

$$\left\{M_s\right\} = \omega^2 m \left[\begin{matrix}\downarrow s \\ \end{matrix}\overrightarrow{\left[x_s - x_r\right]}^{r} - \left\{x_s\right\}\left[1\right]\right]\left[\frac{m_r}{m}\right]\left\{y_r\right\}$$

where $x_s - x_r$ is replaced by zero when $x_r \geqq x_s$ for $s = 1, 2, 3, \ldots p - 1$.

When considering the conditions imposed, the $x_s - x_r$ matrix becomes a triangular matrix as illustrated

$$\begin{bmatrix} 0 & 0 & 0 & \cdots & 0 \\ x_2 - x_1 & 0 & 0 & \cdots & 0 \\ x_3 - x_1 & x_3 - x_2 & 0 & \cdots & 0 \\ x_4 - x_1 & x_4 - x_2 & x_4 - x_3 & \cdots & 0 \\ \vdots & \vdots & x_5 - x_3 & \cdots & 0 \\ \vdots & \vdots & \vdots & \cdots & \vdots \\ \vdots & \vdots & \vdots & & \vdots \\ x_{p-1} - x_1 & x_{p-1} - x_2 & x_{p-1} - x_3 & \cdots & 0 \end{bmatrix}$$

The $\left\{x_s\right\}\left[1\right]$ matrix is

$$\begin{bmatrix} x_1 & x_1 & x_1 & \cdots & x_1 \\ x_2 & x_2 & x_2 & \cdots & x_2 \\ x_3 & x_3 & \cdot & \cdots & x_3 \\ \vdots & \vdots & \vdots & & \vdots \\ \vdots & \vdots & \vdots & \cdots & \vdots \\ \vdots & \vdots & \vdots & & \vdots \\ x_{p-1} & x_{p-1} & \cdot & \cdots & x_{p-1} \end{bmatrix}$$

Subtracting the $\left\{x_s\right\}\left[1\right]$ matrix from the $\left[x_s - x_r\right]$ conditional matrix results in

$$\left\{M_s\right\} = -\omega^2 m \begin{bmatrix} x_1 & x_1 & x_1 & x_1 & x_1 & \cdots & \cdot & x_1 \\ x_1 & x_2 & x_2 & x_2 & x_2 & \cdots & \cdot & x_2 \\ x_1 & x_2 & x_3 & x_3 & x_3 & \cdots & \cdot & x_3 \\ x_1 & x_2 & x_3 & x_4 & x_4 & \cdots & \cdot & x_4 \\ \cdot & \cdot & \cdot & \cdot & \cdot & & \cdot & \cdot \\ \cdot & \cdot & \cdot & \cdot & \cdot & \cdots & \cdot & \cdot \\ \cdot & \cdot & \cdot & \cdot & \cdot & & \cdot & \cdot \\ \cdot & \cdot & \cdot & \cdot & \cdot & \cdots & \cdot & x_{p-2} \\ x_1 & x_2 & x_3 & x_4 & \cdot & \cdots & x_{p-2} & x_{p-1} \end{bmatrix} \left[\frac{m_r}{m}\right]\left\{y_r\right\} = -\omega^2 m \left[X\right]\left[\frac{m_r}{m}\right]\left\{y_r\right\}$$

$$(r = 1, 2, 3 \ldots p - 1) \quad (22)$$

L 1933

Equation (22) conveniently expresses the bending moment at any station in the system except station zero. For a free-free system such as the one being investigated, the moment at the zero station is zero. The $\left[X\right]$ matrix is a symmetrical matrix where all elements to the right and below the diagonal have the same values as their diagonal values; therefore, it is an easy matrix to generate.

Deflection Influence Coefficients

The deflection influence coefficient $\sigma_{r,n}$ is considered as being composed of two contributing parts: the part $\alpha_{r,n}$ due to elementary beam flexure only, and the part $\delta_{r,n}$ due to local rotation.

Deflection influence coefficients due to beam flexure only.- Let $\alpha_{r,n}$ be the deflection at $x = x_r$ due to a unit load at $x = x_n$ considering elementary beam flexure only and cantilevered at $x = 0$. Then consider the following sketch:

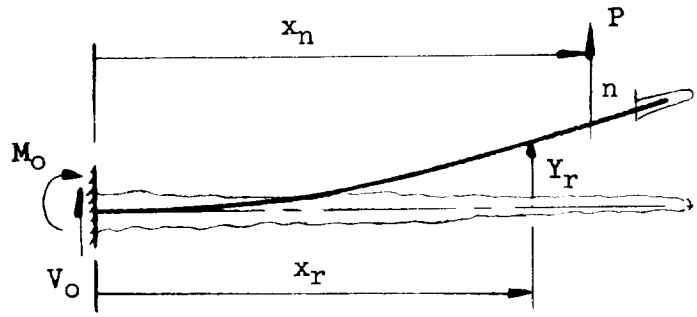

Sketch 2

Then, from sketch 2 when $0 \leqq x \leqq x_n$,

$$EI \frac{d^2y}{dx^2} = M_o + V_o x$$

$$\frac{dy_r}{dx} = M_o \int_0^{x_r} \frac{1}{EI}\, dx + V_o \int_0^{x_r} \frac{x}{EI}\, dx$$

$$y_r = M_o \int_0^{x_r} dx \int_0^{x} \frac{1}{EI}\, dx + V_o \int_0^{x_r} dx \int_0^{x} \frac{x}{EI}\, dx$$

The double integrals can be reduced to single integrals by integrating by parts, that is,

$$\int_0^{x_r} dx \int_0^{x} \frac{1}{EI}\, dx = x_r \int_0^{x_r} \frac{1}{EI}\, dx - \int_0^{x_r} \frac{x}{EI}\, dx$$

and

$$\int_0^{x_r} dx \int_0^{x} \frac{x}{EI}\, dx = x_r \int_0^{x_r} \frac{x}{EI}\, dx - \int_0^{x_r} \frac{x^2}{EI}\, dx$$

By making these substitutions in y_r and noting that

$$M_o = Px_n \qquad V_o = -P \qquad \frac{y_r}{P} = \alpha_{r,n}$$

then,

$$\alpha_{r,n} = \int_0^{x_r} \frac{x^2}{EI}\,dx - \left(x_n + x_r\right)\int_0^{x_r} \frac{x}{EI}\,dx + x_n x_r \int_0^{x_r} \frac{1}{EI}\,dx \qquad (23)$$

$$\left(\text{valid only when } \; x_n \geqq x_r\right)$$

By using the following definitions,

$$\int_0^{x_r} \frac{1}{EI}\,dx = \eta_r \qquad \int_0^{x_r} \frac{x}{EI}\,dx = \mu_r \qquad \int_0^{x_r} \frac{x^2}{EI}\,dx = \beta_r$$

the $\alpha_{r,n}$ coefficient becomes

$$\alpha_{r,n} = \beta_r - \left(x_n + x_r\right)\mu_r + x_n x_r \eta_r \quad (\text{when } \; n \geqq r) \qquad (23a)$$

Equation (23a) is the equation for the deflection influence coefficient of a beam cantilevered at $x = 0$ due to typical beam flexure only.

Equation (23a) is expressed in the matrix form

$$\underset{\downarrow r}{\overset{\rightarrow n}{\left[\alpha_{r,n}\right]}} = \left[\left\langle\left\{\beta_r\right\} - \left[x_r\right]\left\{\mu_r\right\}\right\rangle\left[1\right] + \left\langle\left[x_r\right]\left\{\eta_r\right\} - \left\{\mu_r\right\}\right\rangle\left[x_n\right]\right] \qquad (23b)$$

$$(\text{valid when } \; n \geqq r)$$

According to Maxwell's reciprocal law, the coefficients when $n < r$ can be found immediately, since

$$\alpha_{r,n} = \alpha_{n,r}$$

Therefore equation (23b) is a symmetrical matrix.

Deflection influence coefficients due to joint rotation.- In many fabricated structures the beam analogy might not be adequate to describe local points of high rotation which result from joints or other geometric characteristics. It is therefore desirable to include in the overall influence coefficients terms to allow for slope discontinuities such as those illustrated in the following sketch:

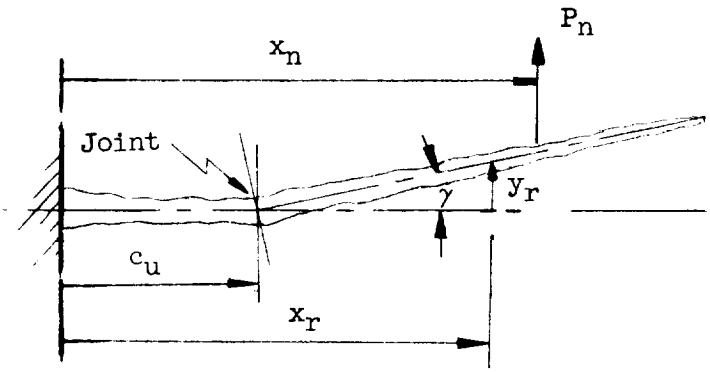

Sketch 3

The rotation at the joint will be defined as a linear function of the moment, that is

$$\gamma = \kappa_u P_n \left(x_n - c_u\right)$$

The deflection at $x = x_r$ due to v such joint rotations resulting from a unit load at $x = x_n$ is

$$\delta_{r,n} = \sum_{u=1}^{v} \kappa_u \left(x_n - c_u\right)\left(x_r - c_u\right) \tag{24}$$

where the product $\left(x_n - c_u\right)\left(x_r - c_u\right)$ under the summation is considered to contribute to the sum only when

$$x_r, x_n \geqq c_u$$

Equation (24) can be expressed as the sum of v separate square matrices, one for each value of u, that is;

$$\overset{\downarrow r}{\overset{\rightarrow n}{\left[\delta^{(u)}_{r,n}\right]}} = \kappa_u \left[\left\{\left\{x_r\right\} - c_u\left\{1\right\}\right\}\left\{\left\{x_n\right\} - c_u\left\{1\right\}\right\}^T\right] \tag{25}$$

where

$$\delta^{(u)}_{r,n} \neq 0 \qquad (\text{when } x_r,\ x_n > c_u)$$

$$\delta^{(u)}_{r,n} = 0 \qquad (\text{when } x_r,\ x_n \leqq c_u)$$

Since the matrix is symmetrical, that is, $\delta^{(u)}_{r,n} = \delta^{(u)}_{n,r}$, only one-half the elements need be computed. The typical appearance of the $\delta^{(u)}_{r,n}$ matrix is

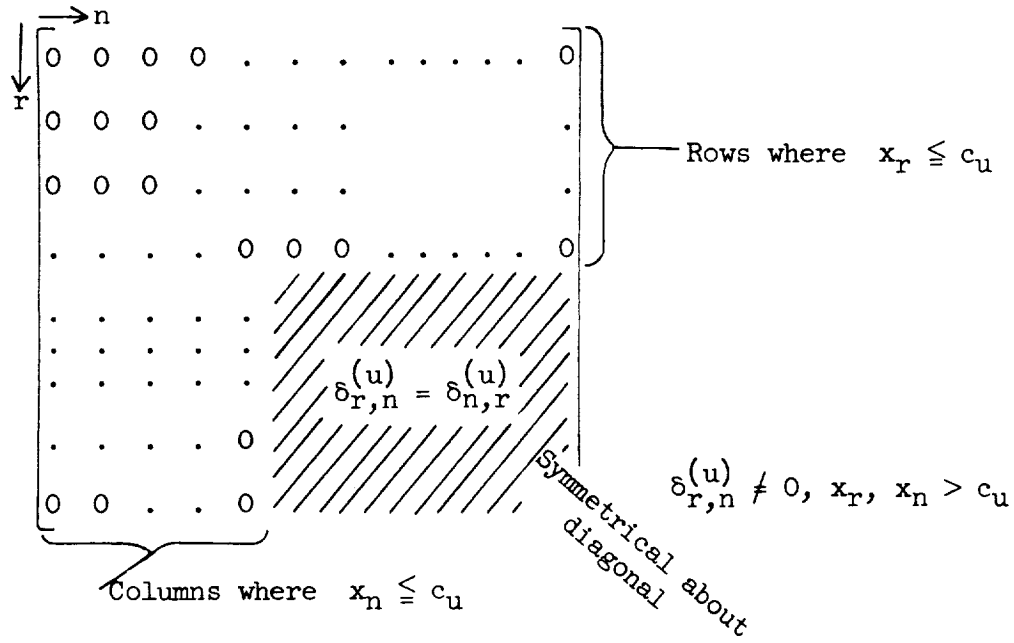

Total deflection influence coefficients.- Addition of the structural flexural influence coefficients and the joint rotation deflection influence coefficients results in the total deflection influence coefficients $\sigma_{r,n}$. Recalling that a structure might possess v joints, then

$$\left[\sigma_{r,n}\right] = \left[\alpha_{r,n}\right] + \left[\delta^{(1)}_{r,n}\right] + \left[\delta^{(2)}_{r,n}\right] + \ldots + \left[\delta^{(v)}_{r,n}\right] \qquad (26)$$

The $\sigma_{r,n}$ matrix is the deflection influence coefficient matrix and is symmetrical about the principal diagonal, thus

$$\sigma_{r,n} = \sigma_{n,r}$$

Slope Influence Coefficients

Mode slopes are of fundamental value in many other studies, particularly those involving airloads on the beam. They are conveniently computed by use of slope influence coefficients as was previously demonstrated by equation (21). As was the case of the deflection influence

coefficients, two contributions to the mode slopes are considered: the slope due to elementary beam flexure, and the effects of a finite rotation at a local point.

Slope influence coefficients due to beam flexure.- Let $\nu_{r,n}$ be the slope at $x = x_r$ due to a unit load at $x = x_n$ due to beam flexure when cantilevered at $x = 0$. Then, from inspection of the following sketch:

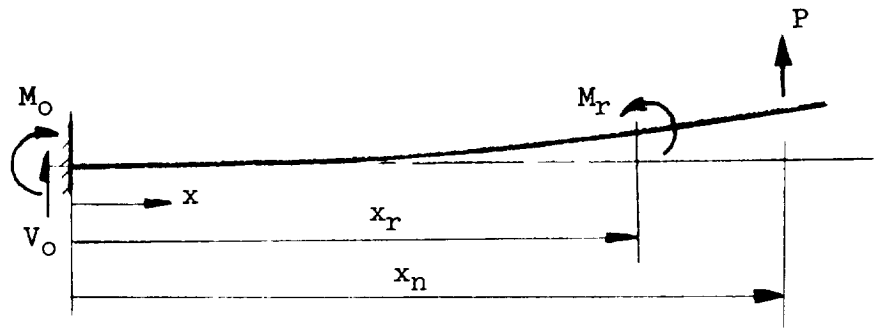

Sketch 4

it is found from summing moments about $x = x_o$

$$M_o - M_r - Px_n = 0$$

and summing vertical forces

$$V_o + P = 0$$

The moment at x in the span where $0 \leqq x \leqq x_r$, is

$$M_x = M_o + V_o x = M_r + Px_n - Px = M_r + P(x_n - x)$$

and the moment at x in the span where $x_r \leqq x \leqq x_n$, is

$$M_x = M_o + V_o x - M_r = P(x_n - x)$$

The total strain energy in the stressed system is

$$U = \int_0^{x_r} \frac{\left[M_r + P(x_n - x)\right]^2}{2EI}\,dx + \int_{x_r}^{x_n} \frac{\left[P(x_n - x)\right]^2}{2EI}\,dx$$

The slope at $x = x_r$ due to the load at $x = x_n$ is

$$\theta_{r,n} = \frac{\partial U}{\partial M_r} = \int_0^{x_r} \frac{M_r + P(x_n - x)}{EI}\, dx$$

from which the influence coefficients are obtained, that is,

$$\nu_{r,n} = \frac{\partial \theta_{r,n}}{\partial P} = \int_0^{x_r} \frac{(x_n - x)}{EI}\, dx = x_n \int_0^{x_r} \frac{1}{EI}\, dx - \int_0^{x_r} \frac{x}{EI}\, dx \qquad (27)$$

(valid when $r \leqq n$)

Since the slope influence coefficient $\nu_{r,n} \neq \nu_{n,r}$, the values of $\nu_{n,r}$ for $r > n$ must also be expressed.

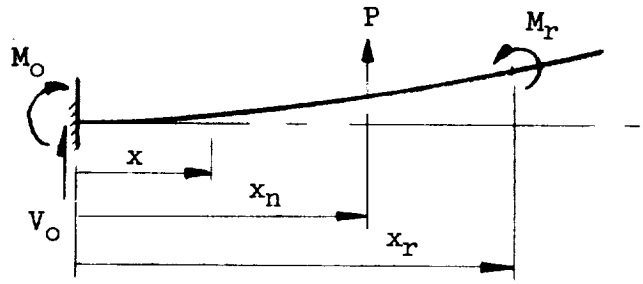

Sketch 5

From inspection of sketch 5 it can be seen that the moment at x in the span where $0 \leqq x \leqq x_n$ is the same as for the preceding case, that is

$$M_x = M_r + P(x_n - x)$$

The moment at x in the span where $x_n \leqq x \leqq x_r$ is

$$M_x = M_o + V_o x + P(x - x_n) = M_r$$

The total strain energy in the stressed system is then

$$U = \int_0^{x_n} \frac{\left[M_r + P(x_n - x)\right]^2}{2EI}\, dx + \int_{x_n}^{x_r} \frac{M_r{}^2 dx}{2EI}$$

The slope at $x = x_r$ due to the load at $x = x_n$ is

$$\theta_{r,n} = \frac{\partial U}{\partial M_r} = \int_0^{x_n} \frac{\left[M_r + P\left(x_n - x\right)\right]}{EI}\, dx + \int_{x_n}^{x_r} \frac{M_r dx}{EI}$$

from which the influence coefficients follow

$$\nu_{r,n} = \frac{\partial \theta_{r,n}}{\partial P} = \int_0^{x_n} \frac{\left(x_n - x\right)}{EI}\, dx = x_n \int_0^{x_n} \frac{1}{EI}\, dx - \int_0^{x_n} \frac{x}{EI}\, dx = \nu_{n,n} \qquad (28)$$

(valid when $r \geqq n$)

L 1933

This result is as would be expected, that for $M_r = 0$, the slope outboard of P, where $x_r > x_n$, is constant at all points and equal to the value at x_n. This result simplifies the problem of determining the $\nu_{r,n}$ matrix coefficients. It simply means that the coefficients in each column below the diagonal have the same values as their diagonal values. This is illustrated as follows:

$$\left[\nu_{r,n}\right] = \begin{array}{c} \\ \downarrow r \end{array} \overset{\longrightarrow n}{\begin{bmatrix} \nu_{1,1} & \nu_{1,2} & \nu_{1,3} & \cdots & \nu_{1,p-1} \\ \nu_{2,1} & \nu_{2,2} & \nu_{2,3} & \cdots & \nu_{2,p-1} \\ \nu_{3,1} & \nu_{3,2} & \nu_{3,3} & \cdots & \nu_{3,p-1} \\ \vdots & \vdots & \vdots & & \vdots \\ \nu_{r,1} & \nu_{r,2} & \cdots & \cdots & \nu_{r,p-1} \\ \vdots & \vdots & \vdots & & \vdots \\ \nu_{p-1,1} & \nu_{p-1,2} & \nu_{p-1,3} & \cdots & \nu_{p-1,p-1} \end{bmatrix}} = \begin{bmatrix} \nu_{1,1} & \nu_{1,2} & \nu_{1,3} & \cdots & \nu_{1,p-1} \\ \nu_{1,1} & \nu_{2,2} & \nu_{2,3} & \cdots & \nu_{2,p-1} \\ \nu_{1,1} & \nu_{2,2} & \nu_{3,3} & \cdots & \nu_{3,p-1} \\ \nu_{1,1} & \nu_{2,2} & \nu_{3,3} & \cdots & \nu_{4,p-1} \\ \vdots & \vdots & \vdots & & \vdots \\ \nu_{1,1} & \nu_{2,2} & \nu_{3,3} & \cdots & \nu_{p-1,p-1} \end{bmatrix} \qquad (28a)$$

Again, using the notation

$$\int_0^{x_r} \frac{1}{EI}\, dx = \eta_r \qquad \int_0^{x_r} \frac{x}{EI}\, dx = \mu_r$$

the influence elements can be expressed as

$$\left.\begin{aligned} \nu_{r,n} &= x_n\eta_r - \mu_r \qquad (r \leqq n) \\ \nu_{r,n} &= \nu_{n,n} = x_n\eta_m - \mu_n \qquad (r > n) \end{aligned}\right\} \tag{28b}$$

and in matrix notation,

$$\left[\nu_{r,n}\right] = \begin{bmatrix} \ddots & & & \\ & \langle\eta_r\rangle[x_n] - \langle\mu_r\rangle[1] & & \\ & & \ddots & \\ & & & \nu_{n,n} \end{bmatrix} = \begin{bmatrix} \eta_1x_1 & \eta_1x_2 & \eta_1x_3 & \cdot & \cdots & \eta_1x_{p-1} \\ \cdot & \eta_2x_2 & \eta_2x_3 & \cdot & \cdots & \eta_2x_{p-1} \\ \cdot & \cdot & \eta_3x_3 & \eta_3x_4 & \cdots & \eta_3x_{p-1} \\ \cdot & \cdot & \cdot & \cdot & & \cdot \\ \cdot & \cdot & \cdot & \cdot & \cdots & \cdot \\ \cdot & \cdot & \cdot & \cdot & & \cdot \\ \eta_1x_1 & \eta_2x_2 & \eta_3x_3 & \cdot & \cdots & \eta_{p-1}x_{p-1} \end{bmatrix}$$

$$- \begin{bmatrix} \mu_1 & \mu_1 & \mu_1 & \cdot & \cdot & \cdots & \mu_1 \\ \mu_1 & \mu_2 & \mu_2 & \mu_2 & \cdot & \cdots & \mu_2 \\ \mu_1 & \mu_2 & \mu_3 & \mu_3 & \mu_3 & \cdots & \mu_3 \\ \cdot & \cdot & \cdot & \cdot & \cdot & & \cdot \\ \cdot & \cdot & \cdot & \cdot & \cdot & \cdots & \cdot \\ \cdot & \cdot & \cdot & \cdot & \cdot & & \cdot \\ \mu_1 & \mu_2 & \mu_3 & \cdot & \cdot & \cdots & \mu_{p-1} \end{bmatrix}$$

Symmetrical about diagonal

$$\mu_{r,n} = \mu_{n,n} = \mu_{n,r} \tag{28c}$$

When the integrals η_r and μ_r have been obtained, the $\nu_{r,n}$ matrix is easily generated in the matrix form of equation (28c).

Slope influence coefficients due to joint rotation.- It is desirable to include in the slope-influence-coefficient equation a term to allow for local rotations. Let $\zeta_{r,n}$ be the slope at $x = x_r$ due to a unit load at $x = x_n$ considering an elastic joint rotation such as that illustrated in the following sketch.

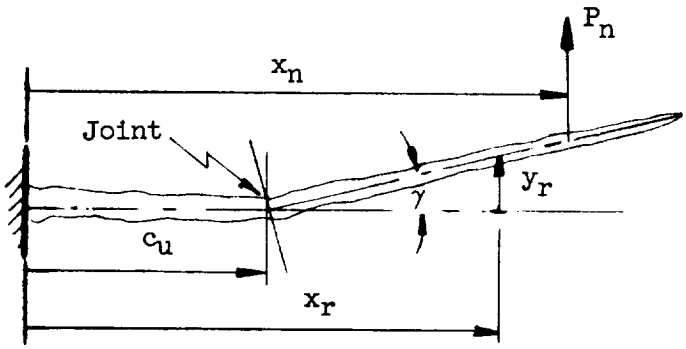

Sketch 6

The moment at the joint $x = c_u$ due to the load P_n is

$$P_n(x_n - c_u)$$

The rotation at the joint will be defined as a linear function of the moment, that is,

$$\gamma = \kappa_u P_n(x_n - c_u)$$

The slope at x_r due to v such joint rotations resulting from a unit load at x_n is

$$\zeta_{r,n} = \sum_{u=1}^{v} \kappa_u(x_n - c_u) \tag{29}$$

where the individual bracketed terms $(x_n - c_u)$ under the summation are included only when $x_n, x_r > c_u$.

Equation (29) can be expressed as the sum of v separate square matrices, one for each value of u.

$$\downarrow r \left[\zeta^{(u)}_{r,n}\right]^{\rightarrow n} = \kappa_u \left\{1\right\}\left\{\left\{x_n\right\} - c_u\left\{1\right\}\right\}^T \qquad \text{(valid when } x_n, x_r > c_u\text{)} \tag{29a}$$

and

$$\zeta^{(u)}_{r,n} = 0 \qquad \text{(when } x_n, x_r \leq c_u\text{)}$$

where all negative elements of the transpose are taken as zero, and all rows when $x_r \leqq c_u$ are to be replaced by zeros.

If a joint coincides with a discrete mass, observing these statements of validity will yield the slope just to the left of the discontinuity resulting from the joint. The magnitude of the discontinuity can be readily computed from the product of the joint rotation factor times the moment at the joint given by equation (22).

The typical appearance of the $\zeta^{(u)}_{r,n}$ matrix is

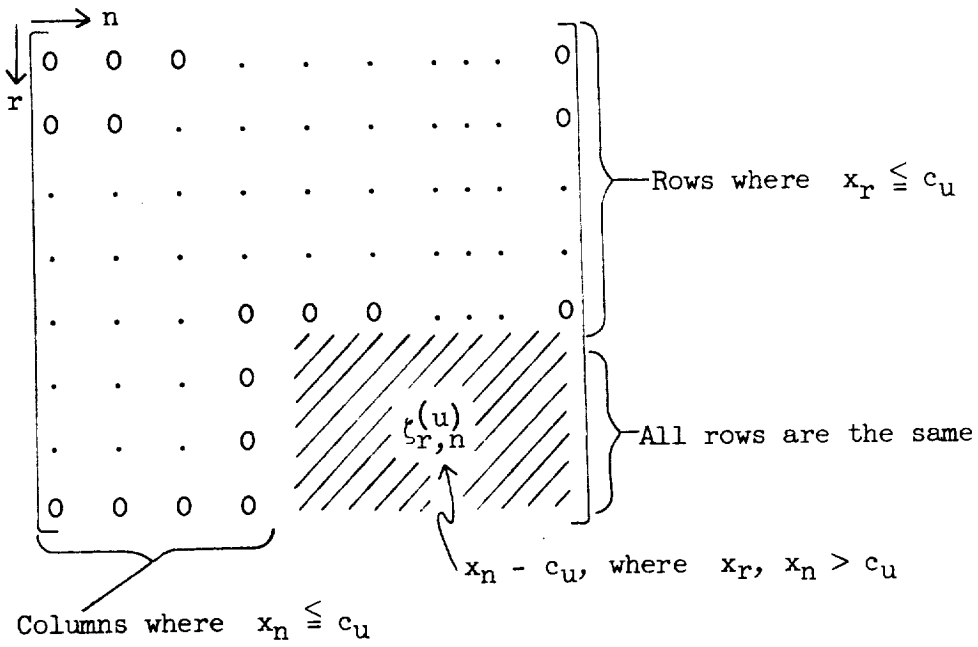

Total slope influence coefficients.- By recalling that $\left[\rho_{n,r}\right]$ is the sum of the flexural coefficients and the joint rotation coefficients, the total slope influence coefficient for a system of v elastic joints is

$$\left[\rho_{r,n}\right] = \left[\nu_{r,n}\right] + \left[\zeta^{(1)}_{r,n}\right] + \left[\zeta^{(2)}_{r,n}\right] + \ldots + \left[\zeta^{(v)}_{r,n}\right] \qquad (30)$$

Equation (30) will yield the values of the slope influence coefficients $\rho_{n,r}$.

Evaluation of Integrals With Treatment of Discontinuities

The $\frac{1}{EI}$ function in the β_r, μ_r, and η_r integrals is for most practical problems a highly discontinuous function, and therefore a numerical form of integration is generally expedient. A system which is convenient for tabulation and readily adaptable to automatic digital computers is outlined as follows:

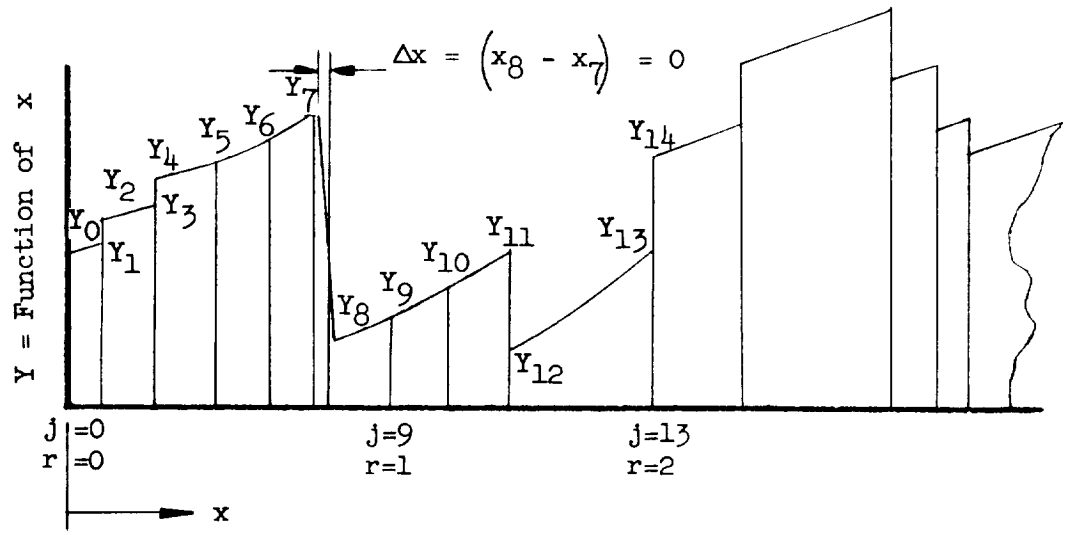

Sketch 7.- Typical curve to be integrated.

The β_r, μ_r, and η_r integrals are definite integrals and need to be evaluated for all designated values of r. In practical cases the integrands of β_r, μ_r, or η_r should be described at many intermediate points to the r subscript system. By introducing a j subscript system for intermediate points and letting j_r be the value of j at the rth station, then from inspection of the preceding sketch the area between $j = 0$ and $j = j_r$ is

$$\int_0^{x_r} Y\,dx = \sum_{j=1}^{j_r} \frac{(Y_j + Y_{j-1})(x_j - x_{j-1})}{2} \tag{31}$$

Notice in sketch 7 that each discontinuity is described with two ordinates and the stations where there are no discontinuities are

defined with only one ordinate. The discontinuity can be considered simply as two adjacent stations with a spacing that approached zero. Thus, no special treatment need be given discontinuities except that the data be supplied with two ordinates at a discontinuity with each having the same x value. Therefore, in equation (31), $(x_j - x_{j-1})$ across a discontinuity will be zero and no change will occur in the integral. As an illustration, a listing of stiffness data and the designation of integration limit for evaluating β_r, μ_r, and η_r for a typical research launch vehicle is furnished as table I. The engineer should adequately describe the Y_j function to minimize numerical integration errors and to represent better the actual physical problem.

Equation (31) is sufficient for evaluating the η_r, μ_r, and β_r integrals by letting the function Y_j represent the integrands $\frac{1}{EI}$, $\frac{x}{EI}$, and $\frac{x^2}{EI}$, respectively.

GENERAL DISCUSSION AND RESULTS

In the foregoing discussion the equations for obtaining the natural mode data of a free-free structure have been derived and presented. A general discussion of the problems encountered in the application of the equations is presented in the following paragraphs and two example solutions are included to illustrate the method. Results of a study to ascertain the accuracies of the calculated natural frequencies and mode shapes and their dependence on the number of masses employed are also furnished.

Choice of the x Origin

The selection of the origin of the x coordinate at the location of m_o was based upon several factors which primarily arose from past applications of the method to multistage rocket vehicles. For multistage vehicles where it is desired to obtain the frequencies and modes for the combinations of stages, it at first appears expedient to choose the x origin at or near the nose of the uppermost stage. This choice permits the use of input data developed for the combined stages for the cases of fewer stages. However, this choice of the x origin, while being most efficient from a work standpoint, has an inherent disadvantage of reduced accuracy. Because the tip of the vehicle is usually the region of greatest flexibility and the influence coefficients and boundary values, y_o and θ_o, are referenced to the x origin, the

choice of the origin at the nose introduces unnecessarily large boundary corrections $(y_o$ and $\theta_o)$ which reduce the accuracy and sometimes affect the numerical solution for the higher modes. These problems can be eliminated in most cases by choosing the x origin at the more rigid end of the vehicle.

In cases where the vehicle is already constructed at the time of analysis, the choice of the origin at the base of the vehicle in many cases has a second advantage of permitting direct measurement of the influence coefficients. Since the coupling hardware for combining the stages can in many cases be used for mounting the missile on a bed plate or back stop, the influence coefficients can be directly measured by using simple dial gages and moderate applied forces. On the other hand, the average rocket vehicle could not be readily supported as a cantilever from its nose.

Locations of Mass Stations

It has also been observed that the positions of the mass stations should be determined by giving primary consideration to the purpose for which the mode data are likely to be used. Experience has indicated that to minimize the reworking of input data, the selection of mass stations should be strongly influenced by the aerodynamic-load distributions. For example, if the influence coefficients and associated modal data are to be employed for gust response studies, it is important that the reference stations be logically located to represent the points of large localized aerodynamic lifting loads. Likewise, it is desirable to choose stations at the centers of pressure of lifting appendages.

Order of the Characteristic Matrix

The selection of the number of discrete masses to represent the continuous system will establish the order of the matrix solution. A system of p masses will necessitate the solution of a matrix of order $p - 1$. The number of masses used should be based primarily on the accuracy desired for the highest mode to be extracted and the available computing capability to handle large matrix iterations.

The results of a study of the influence of the number of masses on the errors in frequencies and mode shapes of a uniform free-free beam are presented in figures 1 and 2. The method derived herein for the cases treated yielded frequencies higher than the comparative classical solutions. The increase in frequency over the comparative classical solution for the case of the uniform beam is shown in figure 1 as the percentage error due to the discrete mass representation. An inspection

of a cross plot of these data for a 1-percent error shows a close correlation between the data and a simple analytical expression. Consequently, it is suggested that an error in frequency not greater than 1 percent can be maintained by the use of the following approximate rule:

$$p = 13\sqrt[3]{n} \qquad (1 \leq n \leq 5)$$

where n is the number of the highest mode desired and p is the number of masses to be used in representing the system. The discrepancies between the computed mode shapes and the classical mode shapes are shown as figure 2. These data show the largest of the errors between like modes at the points of the maximum deflections. The modal differences were determined after alining the two comparative curves to yield the least possible error by the method of least squares. The comparison was made strictly on the basis of the agreement between the shapes of the computed modes and the classical modes for the free-free uniform beam. In order to provide a wide freedom in alining the computed and comparative data, the classical mode shape was permitted to be translated and rotated as necessary in the alinement to provide a minimum to the sum of the squares of the differences between the shapes. The reference curve was expressed as

L 1 9 3 3

$$q_i = a + b\left(x_i - \bar{x}\right) + c\zeta\left(x_i\right)$$

where a, b, and c are coordinates permitting a wide freedom in the placement of the comparative function q_i, and $\zeta(x_i)$ is the classical modal deflection at x_i used as a measure of the accuracy.

An inspection of figure 2 shows that errors in mode shape not in excess of 1 percent through the third mode can be expected with the use of 21 discrete masses in the solution.

It should be recalled that the analysis of the errors due to the number of masses used is applicable specifically to the uniform beam, yet these data are included to be used as a guide in working with unsymmetrical beams and are felt to be indicative of the sensitivity of the method to the number of masses used.

Numerical Integration Errors

An investigation of the errors associated with the integration process given in the section entitled, "Evaluation of Integrals With

Treatment of Discontinuities" has also been made. The variations in the natural frequencies of a 26-mass representation of a uniform beam were computed for evenly spaced EI intervals numbering 25, 50, 100, 150, and 200; and the resulting errors are recorded in figure 3. It is interesting to note that the integration errors introduced by the trapezoidal process tend to counteract the errors introduced by the discrete mass analogy. In the data of figure 3, the root-mean-square values of the errors for the set of five modes show that the optimum compensation of errors for the set of modes is experienced for the case studied with 50 integration intervals. Extending the integration intervals to 200 or more will virtually remove all significant integration errors. This is apparent in figure 3 by the fact that the curves approach a constant value for the larger number of integration intervals. The integration error becomes of decreasing significance as the number of masses are reduced by virtue of its becoming of secondary importance in comparison with the increasingly significant error associated with lumping.

The data for the curves of figure 1 were computed using 100 evenly spaced integration intervals. From the indications of figure 3, it is apparent that some shifting of the ϵ_f values of figure 1 would occur with change in the number of integration intervals. This shifting is of only practical significance when dealing with errors of 1 percent or less. The sensitivity of the data of figure 1 to integration intervals is noted by the comparisons of ϵ_f for 100 and 200 interval integrations given on the figure for $p = 26$. The comparison suggests that no major changes in error would result due to increasing the number of integration intervals beyond 100.

Slope Discontinuities

When flexibilities exist of the nature of local joint rotations, the mode slopes will exhibit discontinuities at each joint of the magnitude of

$$\gamma = \kappa_u M_u$$

where κ_u is the joint rotation constant at the joint u, M_u is the mode moment at u, and γ is the magnitude of the slope discontinuity.

In the event of a joint occurring at one of the mass stations, the slope for the station is then double valued, having one magnitude just to the left of the station and one value to the right. The foregoing equations have been designed to yield only the slope to the left of

the joint in cases where the joint location and station positions are coincident. In order to determine the slope to the right, the magnitude of the discontinuity is readily determined by the above equation for γ. This treatment of discontinuities is clearly illustrated in figure 4.

Shear deformations will also yield slope discontinuities in structures possessing discontinuities in shear stiffness. If extreme accuracy is required in the definitions of mode slopes and if shear deformation is thought to be a significant contributor to deflection, then the subject method should either be extended to include shear effects or be discarded in favor of methods more suitable for treating secondary influences.

NUMERICAL EXAMPLES

Two numerical illustrations of portions of the foregoing derivations are submitted in order to show more clearly the procedures and to demonstrate the simplicity of the method presented. A solution of the classical case of the free-free vibration of a uniform beam is given and a detailed application of the method to a typical rocket vehicle is shown.

Free-Free Uniform Beam

Consider the following representation of a uniform beam of total mass m and overall length L.

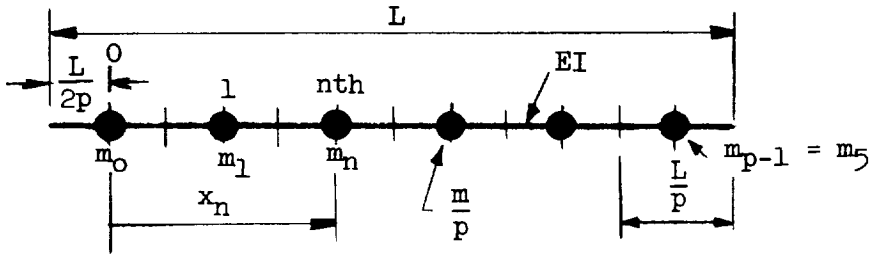

Sketch 8.- The p mass system of a uniform beam.

For the equally divided span, the six segments are represented by six equal discrete masses (p = 6), thus

$$m_n = \frac{m}{6}$$

$$x_n = \frac{L}{6} n$$

$$\bar{x} = \frac{L(p - 1)}{2p} = \frac{5}{12} L$$

$$\bar{r}^2 = \frac{\sum_0^5 m_n x_n^2}{\sum_0^5 m_n} - \bar{x}^2 = \frac{55L^2}{6 \times 36} - \frac{25L^2}{144} = \frac{35L^2}{432}$$

L
1
9
3
3

and

$$\frac{\bar{x}^2}{\bar{r}^2} = \frac{15}{7}$$

Utilizing the above quantities and relationships, the various matrices of equation (10) can be evaluated and result in the following expressions.

$$\left\{\frac{x_r}{\bar{x}}\right\} = \frac{2}{5}\begin{Bmatrix} 1 \\ 2 \\ 3 \\ 4 \\ 5 \end{Bmatrix}$$

$$\left[1 - \frac{x_r}{\bar{x}}\right] = \frac{1}{5}\begin{bmatrix} 3 & 1 & -1 & -3 & -5 \end{bmatrix}$$

$$\left[1 + \frac{\bar{x}^2}{\bar{r}^2} - \frac{\bar{x}^2}{\bar{r}^2}\frac{x_r}{\bar{x}}\right] = \frac{1}{7}\begin{bmatrix} 16 & 10 & 4 & -2 & -8 \end{bmatrix}$$

$$\left[\frac{m_r}{m}\right] = \frac{1}{6}\begin{bmatrix} 1 & & & & \\ & 1 & & & \\ & & 1 & & \\ & & & 1 & \\ & & & & 1 \end{bmatrix}$$

With the preceding matrices, the premultiplier of the $\sigma_{r,n}$ matrix of equation (10) can be written

$$\left[\left[1\right] + \left[\frac{\bar{x}^2}{\bar{r}^2}\left\{\frac{x_r}{\bar{x}}\right\}\left[1 - \frac{x_r}{\bar{x}}\right] - \left\{1\right\}\left[1 + \frac{\bar{x}^2}{\bar{r}^2} - \frac{\bar{x}^2}{\bar{r}^2}\frac{x_r}{\bar{x}}\right]\right]\left[\frac{m_r}{m}\right]\right]$$

$$= \frac{1}{210}\begin{bmatrix} 148 & -44 & -26 & -8 & 10 \\ -44 & 172 & -32 & -26 & -20 \\ -26 & -32 & 172 & -44 & -50 \\ -8 & -26 & -44 & 148 & -80 \\ 10 & -20 & -50 & -80 & 100 \end{bmatrix}$$

When EI can be assumed constant as in the case of the uniform beam, equation (23) can be easily expressed analytically as

$$\alpha_{r,n} = \frac{1}{EI}\left(\int_0^{x_r} x^2\,dx - \left(x_n + x_r\right)\int_0^{x_r} x\,dx + x_n x_r \int_0^{x_r} dx\right)$$

$$= \frac{x_r^2}{2EI}\left(x_n - \frac{x_r}{3}\right)$$

$$= \left(\frac{L}{6}\right)^3 \frac{r^2}{6EI}(3n - r) \qquad (n \geqq r)$$

and $\alpha_{r,n} = \alpha_{n,r}$ when $n < r$. Upon evaluation of the previous equation for the appropriate combinations of n and r between 1 and 5 and arranging the results in matrix form, the following matrix for $\alpha_{r,n}$ results

$$\left[\alpha_{r,n}\right] = \frac{L^3}{6^4 EI} \begin{array}{c} \\ r \downarrow \end{array} \overset{\longrightarrow n}{\begin{bmatrix} 2 & 5 & 8 & 11 & 14 \\ 5 & 16 & 28 & 40 & 52 \\ 8 & 28 & 54 & 81 & 108 \\ 11 & 40 & 81 & 128 & 176 \\ 14 & 52 & 108 & 176 & 250 \end{bmatrix}}$$

L
1
9
3
3

By assuming that the uniform beam is free of any local joint flexibilities, then

$$\alpha_{r,n} = \sigma_{r,n}$$

and the A matrix can be written as

$$\left[A\right] = \frac{L^3}{35 \times 6^6 EI} \begin{bmatrix} 148 & -44 & -26 & -8 & 10 \\ -44 & 172 & -32 & -26 & -20 \\ -26 & -32 & 172 & -44 & -50 \\ -8 & -26 & -44 & 148 & -80 \\ 10 & -20 & -50 & -80 & 100 \end{bmatrix} \begin{bmatrix} 2 & 5 & 8 & 11 & 14 \\ 5 & 16 & 28 & 40 & 52 \\ 8 & 28 & 54 & 81 & 108 \\ 11 & 40 & 81 & 128 & 176 \\ 14 & 52 & 108 & 176 & 250 \end{bmatrix} \begin{bmatrix} 1 & & & & \\ & 1 & & & \\ & & 1 & & \\ & & & 1 & \\ & & & & 1 \end{bmatrix}$$

$$= \frac{L^3}{35 \times 6^6 EI} \begin{bmatrix} -80 & -492 & -1020 & -1502 & -1932 \\ -50 & -444 & -1530 & -3044 & -4704 \\ -20 & -186 & -780 & -2066 & -3696 \\ 10 & 72 & 180 & 172 & -168 \\ 40 & 330 & 1140 & 2620 & 4620 \end{bmatrix}$$

The solution of equation (10) for the uniform beam is now reduced to the matrix iteration of

$$\frac{35 \times 6^6 EI}{\omega^2 mL^3} \left\{ y \right\} = \begin{bmatrix} -80 & -492 & -1020 & -1502 & -1932 \\ -50 & -444 & -1530 & -3044 & -4704 \\ -20 & -186 & -780 & -2066 & -3696 \\ 10 & 72 & 180 & 172 & -168 \\ 40 & 330 & 1140 & 2620 & 4620 \end{bmatrix} \left\{ y \right\}$$

The dominant characteristic value and characteristic function of the preceding matrix equation will yield the first natural frequency and first natural mode shape, respectively, of the free-free uniform beam as represented by sketch 8. Proceeding by matrix iteration, six iterations of an initially assumed modal column of 0.2, -0.2, -0.2, 0.2, and 1.0 will yield first mode amplitudes and frequencies to an accuracy better than one-tenth of 1 percent of the fully converged results. The mode shape and frequency so obtained are

$$\frac{35 \times 6^6 EI}{\omega^2 mL^3} = 2986.3 \qquad \omega = 23.385 \sqrt{\frac{EI}{mL^3}}$$

$$y_n = \begin{Bmatrix} -0.13744 \\ -0.86256 \\ -0.86256 \\ -0.13741 \\ 1.00000 \end{Bmatrix} \qquad f = 3.72 \sqrt{\frac{EI}{mL^3}}$$

From equation (11), y_o is

$$y_o = -\begin{bmatrix}1\end{bmatrix}\begin{bmatrix}1 & & & & \\ & 1 & & & \\ & & 1 & & \\ & & & 1 & \\ & & & & 1\end{bmatrix}\begin{Bmatrix}-0.13744\\ -0.86256\\ -0.86256\\ -0.13741\\ 1.00000\end{Bmatrix} = 0.99997$$

Should a joint of κ_1 flexibility be considered at the third mass position, for example, the $\delta^{(1)}_{r,n}$ matrix would need to be considered. By substituting the following into equation (25),

$$x_r = \frac{L}{6}\,r \qquad x_n = \frac{L}{6}\,n \qquad c_u = \frac{L}{3}$$

it then becomes

$$\delta^{(1)}_{r,n} = \frac{\kappa_1 L^2}{36}\begin{array}{c} \\ \downarrow r \end{array}\begin{array}{c}\longrightarrow n\end{array}\begin{bmatrix} 0 & 0 & 0 & 0 & 0 \\ 0 & 0 & 0 & 0 & 0 \\ 0 & 0 & 1 & 2 & 3 \\ 0 & 0 & 2 & 4 & 6 \\ 0 & 0 & 3 & 6 & 9 \end{bmatrix}$$

and the total influence coefficient with the joint included would be

$$\sigma_{r,n} = \alpha_{r,n} + \delta^{(1)}_{r,n}$$

$$= \frac{L^3}{6^4 EI}\left[\begin{bmatrix} 2 & 5 & 8 & 11 & 14 \\ 5 & 16 & 28 & 40 & 52 \\ 8 & 28 & 54 & 81 & 108 \\ 11 & 40 & 81 & 128 & 176 \\ 14 & 52 & 108 & 176 & 250 \end{bmatrix} + \frac{\kappa_1 EI 6^2}{L}\begin{bmatrix} 0 & 0 & 0 & 0 & 0 \\ 0 & 0 & 0 & 0 & 0 \\ 0 & 0 & 1 & 2 & 3 \\ 0 & 0 & 2 & 4 & 6 \\ 0 & 0 & 3 & 6 & 9 \end{bmatrix}\right]$$

L
1
9
3
3

Let $\frac{\kappa_1 EI 6^2}{L} = 4$; the A matrix becomes

$$\left[A\right] = \frac{L^3}{35 \times 6^6 EI}\begin{bmatrix} 148 & -44 & -26 & -8 & 10 \\ -44 & 172 & -32 & -26 & -20 \\ -26 & -32 & 172 & -44 & -50 \\ -8 & -26 & -44 & 148 & -80 \\ 10 & -20 & -50 & -80 & 100 \end{bmatrix}\begin{bmatrix} 2 & 5 & 8 & 11 & 14 \\ 5 & 16 & 28 & 40 & 52 \\ 8 & 28 & 58 & 89 & 120 \\ 11 & 40 & 89 & 144 & 200 \\ 14 & 52 & 120 & 200 & 286 \end{bmatrix}$$

$$= \frac{L^3}{35 \times 6^6 EI}\begin{bmatrix} -80 & -492 & -1068 & -1598 & -2076 \\ -50 & -444 & -2106 & -4196 & -6432 \\ -20 & -186 & -1044 & -2594 & -4488 \\ 10 & 72 & 228 & 268 & -24 \\ 40 & 330 & 1500 & 3340 & 5700 \end{bmatrix}$$

and the lowest natural frequency and mode shape obtained for the case with the joint are

$$\omega = \sqrt{\frac{35 \times 6^6 EI}{3832.9mL^3}} = 20.641\sqrt{\frac{EI}{mL^3}} \qquad f = 3.285\sqrt{\frac{EI}{mL^3}}$$

$$y_n = \begin{Bmatrix} -0.14170 \\ -1.00995 \\ -0.83797 \\ -0.08112 \\ 1.00000 \end{Bmatrix} \qquad y_o = 1.07074$$

The mode slopes (dy/dx) are computed by equations (8) and (21). With the utilization of the previously developed matrices, the boundary values θ_o for the cases with and without joints are readily obtained.

For the case without a joint,

$$\theta_o = \frac{36}{2986.3L} \begin{Bmatrix} 3 \\ 1 \\ -1 \\ -3 \\ -5 \end{Bmatrix}^T \begin{bmatrix} 1 & & & & \\ & 1 & & & \\ & & 1 & & \\ & & & 1 & \\ & & & & 1 \end{bmatrix} \begin{bmatrix} 2 & 5 & 8 & 11 & 14 \\ 5 & 16 & 28 & 40 & 52 \\ 8 & 28 & 54 & 81 & 108 \\ 11 & 40 & 81 & 128 & 176 \\ 14 & 52 & 108 & 176 & 250 \end{bmatrix} \begin{bmatrix} 1 & & & & \\ & 1 & & & \\ & & 1 & & \\ & & & 1 & \\ & & & & 1 \end{bmatrix} \begin{Bmatrix} -0.13744 \\ -0.86256 \\ -0.86256 \\ -0.13741 \\ 1.00000 \end{Bmatrix} = -\frac{7.2472}{L}$$

For the case with the assumed joint at $x = c_u = L/3$,

$$\theta_o = \frac{36}{3832.9L} \begin{Bmatrix} 3 \\ 1 \\ -1 \\ -3 \\ -5 \end{Bmatrix}^T \begin{bmatrix} 1 & & & & \\ & 1 & & & \\ & & 1 & & \\ & & & 1 & \\ & & & & 1 \end{bmatrix} \begin{bmatrix} 2 & 5 & 8 & 11 & 14 \\ 5 & 16 & 28 & 40 & 52 \\ 8 & 28 & 58 & 89 & 120 \\ 11 & 40 & 89 & 144 & 200 \\ 14 & 52 & 120 & 200 & 286 \end{bmatrix} \begin{bmatrix} 1 & & & & \\ & 1 & & & \\ & & 1 & & \\ & & & 1 & \\ & & & & 1 \end{bmatrix} \begin{Bmatrix} -0.14170 \\ -1.00995 \\ -0.83797 \\ -0.08112 \\ 1.00000 \end{Bmatrix} = -\frac{7.6272}{L}$$

The slopes at stations other than $n = 0$ require knowledge of the slope influence coefficients. From equation (27), it may be observed that the slope influence coefficients due to flexure only can be expressed, when $r \leqq n$, as

$$\nu_{r,n} = x_n \int_0^{x_r} \frac{1}{EI}\, dx - \int_0^{x_r} \frac{x}{EI}\, dx$$

For the case of constant EI and when $x_n = \frac{Ln}{6}$ or $x_r = \frac{Lr}{6}$,

$$\nu_{r,n} = \frac{1}{2EI}\left(\frac{L}{6}\right)^2 r(2n - r) \qquad (r \leqq n)$$

L 1933

It should be noted, as previously mentioned, that the slope influence coefficients are not symmetrical, that is, $\nu_{r,n} \neq \nu_{n,r}$; yet $\nu_{r,n}$ when $r \geqq n$ can be easily found by the relationship

$$\nu_{r,n} = \nu_{n,n}$$

The slope influence coefficients for flexure only for all combinations of r and n from 1 to 5 are then given by

$$\nu_{r,n} = \frac{L^2}{6^3 EI} \begin{array}{c} \\ r\downarrow \\ \\ \\ \\ \end{array} \begin{array}{c} \overset{n\rightarrow}{\begin{bmatrix} 3 & 9 & 15 & 21 & 27 \\ 3 & 12 & 24 & 36 & 48 \\ 3 & 12 & 27 & 45 & 63 \\ 3 & 12 & 27 & 48 & 72 \\ 3 & 12 & 27 & 48 & 75 \end{bmatrix}} \end{array}$$

For the case without joints $\rho_{r,n} = \nu_{r,n}$. Since the solution for the characteristic value $\frac{m\omega^2 L^3}{EI} = \frac{35 \times 6^6}{2986.3}$, the slopes for all stations for the case without the joint can be found from equation (21) as

$$L\left\{\theta_r\right\} = \frac{36}{2986.3}\left[\begin{Bmatrix}1\\1\\1\\1\\1\end{Bmatrix}\begin{Bmatrix}3\\1\\-1\\-3\\-5\end{Bmatrix}^T\begin{bmatrix}1&&&&\\&1&&&\\&&1&&\\&&&1&\\&&&&1\end{bmatrix}\begin{bmatrix}2&5&8&11&14\\5&16&28&40&52\\8&28&54&81&108\\11&40&81&128&176\\14&52&108&176&250\end{bmatrix}\right.$$

$$\left. + 35\begin{bmatrix}3&9&15&21&27\\3&12&24&36&48\\3&12&27&45&63\\3&12&27&48&72\\3&12&27&48&75\end{bmatrix}\right]\begin{bmatrix}1&&&&\\&1&&&\\&&1&&\\&&&1&\\&&&&1\end{bmatrix}\begin{Bmatrix}-0.13744\\-0.86256\\-0.86256\\-0.13741\\1.00000\end{Bmatrix} = \begin{Bmatrix}-5.9811\\-2.3576\\2.3577\\5.9811\\7.2469\end{Bmatrix}$$

In the event that the structure has a joint, the $\nu_{r,n}$ matrix as shown previously must be combined with the $\zeta_{r,n}$ matrix of equation (29a). As for the previous example, assume that a joint exists at the third mass station, station 2, which has a joint constant of $\kappa_1 = \frac{4L}{6^2EI}$ and position of $c_u = \frac{L}{3}$. Then, from equation (29a), it follows that

$$\overset{\rightarrow n}{\underset{r}{\downarrow}}\left[\zeta^{(1)}_{r,n}\right] = \frac{4L^2}{6^3EI}\begin{Bmatrix}1\end{Bmatrix}\left\{\begin{Bmatrix}1\\2\\3\\4\\5\end{Bmatrix} - \begin{Bmatrix}2\\2\\2\\2\\2\end{Bmatrix}\right\}^T$$

and since all coefficients are zero except those where $n,r > 2$, then

$$\left[\zeta_{r,n}^{(1)}\right] = \frac{4L^2}{6^3 EI}\begin{bmatrix} 0 & 0 & 0 & 0 & 0 \\ 0 & 0 & 0 & 0 & 0 \\ 0 & 0 & 1 & 2 & 3 \\ 0 & 0 & 1 & 2 & 3 \\ 0 & 0 & 1 & 2 & 3 \end{bmatrix}$$

Addition of these results to the $\nu_{r,n}$ matrix results in the slope influence coefficient matrix which contains both the flexural and joint contributions, namely,

L 1933

$$\left[\rho_{r,n}\right] = \frac{L^2}{6^3 EI}\begin{array}{c} \\ r\downarrow \end{array}\overset{\begin{array}{ccccc} & & & & n\rightarrow \end{array}}{\begin{bmatrix} 3 & 9 & 15 & 21 & 27 \\ 3 & 12 & 24 & 36 & 48 \\ 3 & 12 & 31 & 53 & 75 \\ 3 & 12 & 31 & 56 & 84 \\ 3 & 12 & 31 & 56 & 87 \end{bmatrix}}$$

The mode slopes at all stations are then obtained from equation (21) for the case with the joint as

$$L\left\{\theta_r\right\} = \frac{36}{3832.9}\left[\begin{Bmatrix} 1 \\ 1 \\ 1 \\ 1 \\ 1 \end{Bmatrix}\begin{Bmatrix} 3 \\ 1 \\ -1 \\ -3 \\ -5 \end{Bmatrix}^T\begin{bmatrix} 1 & & & & \\ & 1 & & & \\ & & 1 & & \\ & & & 1 & \\ & & & & 1 \end{bmatrix}\begin{bmatrix} 2 & 5 & 8 & 11 & 14 \\ 5 & 16 & 28 & 40 & 52 \\ 8 & 28 & 58 & 89 & 120 \\ 11 & 40 & 89 & 144 & 200 \\ 14 & 52 & 120 & 200 & 286 \end{bmatrix}\right.$$

$$\left. + 35\begin{bmatrix} 3 & 9 & 15 & 21 & 27 \\ 3 & 12 & 24 & 36 & 48 \\ 3 & 12 & 31 & 53 & 75 \\ 3 & 12 & 31 & 56 & 84 \\ 3 & 12 & 31 & 56 & 87 \end{bmatrix}\right]\begin{bmatrix} 1 & & & & \\ & 1 & & & \\ & & 1 & & \\ & & & 1 & \\ & & & & 1 \end{bmatrix}\begin{Bmatrix} -0.14170 \\ -1.00995 \\ -0.83797 \\ -0.08112 \\ 1.00000 \end{Bmatrix} = \begin{Bmatrix} -6.5713 \\ -3.5431 \\ 2.9511 \\ 5.8297 \\ 6.8159 \end{Bmatrix}$$

The mode moments are readily computed from equation (22). Since the moment equation is of elementary construction, it simply follows for the case of the uniform and equally spaced masses that for the case without a joint,

$$\frac{L^2}{EI}\{M_s\} = -\frac{35 \times 6^4}{2986.3}\begin{bmatrix}1&1&1&1&1\\1&2&2&2&2\\1&2&3&3&3\\1&2&3&4&4\\1&2&3&4&5\end{bmatrix}\begin{bmatrix}1&&&&\\&1&&&\\&&1&&\\&&&1&\\&&&&1\end{bmatrix}\begin{Bmatrix}-0.13744\\-0.86256\\-0.86256\\-0.13741\\1.00000\end{Bmatrix} = \begin{Bmatrix}15.19\\28.29\\28.29\\15.19\\0\end{Bmatrix}$$

L
1
9
3
3

and for the case with the assumed joint at $x = c_u = L/3$

$$\frac{L^2}{EI}\{M_s\} = -\frac{35 \times 6^4}{3832.9}\begin{bmatrix}1&1&1&1&1\\1&2&2&2&2\\1&2&3&3&3\\1&2&3&4&4\\1&2&3&4&5\end{bmatrix}\begin{bmatrix}1&&&&\\&1&&&\\&&1&&\\&&&1&\\&&&&1\end{bmatrix}\begin{Bmatrix}-0.14170\\-1.00995\\-0.83797\\-0.08112\\1.00000\end{Bmatrix} = \begin{Bmatrix}12.67\\23.66\\22.71\\11.83\\0\end{Bmatrix}$$

The mode shapes, mode slopes, and mode moments calculated above for the illustrative case of a uniform beam are displayed on figure 4 for both of the cases; with and without the joint.

Modal Data for a Typical Space Vehicle

In figure 5 a 22 discrete mass representation is shown of an actual space vehicle for which the first three natural modes, their slopes, and moments are furnished as an illustration. The discrete masses are considered to act at the center of gravity of the distributed masses which they represent. From figures 1 and 2, it is estimated that the 22 discrete masses should adequately represent the vehicle's distributed mass to yield data on the first three lowest modes with errors of less than 1 percent.

In table I the flexural coefficients EI are recorded in a convenient form for expediting the required integrations in accordance with the trapezoidal process noted previously. One hundred fifty-six integration stations are supplied to insure negligible integration errors. All discontinuities are included by simply recording both quantities for their common x value. The x values on table I marked with a footnote are the locations of the mass centers and are the integration limits at which the integrals are required for the influence coefficients. In table II, joint rotation constants and their locations are furnished for the inclusion of joint effects in the example vehicle.

The data of figure 5 and tables I and II constitute the necessary input data to calculate the natural frequencies and other modal data for the vehicle. From these data, the first three modes, their slopes, and moments for the example vehicle have been computed and are furnished as figures 6, 7, and 8. The data are given for the vehicle with and without joint effects. The magnitudes of the discontinuities in the slope curves are equal to the products of their respective joint rotation constants and bending moments. All of the modes have been normalized at the 22nd mass and the moments are applicable to the unit deflection of the normalized modes.

CONCLUDING REMARKS

A coordinated matrix approach to the problem of free-free vibrations of unsymmetrical beam-like structures has been presented.

In the application of the method it has been found advantageous to choose the origin of the independent variable x at the discrete mass on the more rigid end.

The choice of the positions of the discrete masses should be dictated by the ultimate use of the modal data to be obtained and in consideration of the actual physical properties of the structure.

The number of discrete masses should be selected to maintain the mode shape and frequency errors within the limits desired. From considerations on uniform beams it is indicated that errors in frequency of 1 percent or less can generally be maintained for the first five modes by the use of the following approximate rule:

$$p = 13\sqrt[3]{n}$$

where n is the number of the highest mode desired and p is the number of masses to use in representing the system. Errors in the mode shapes can generally be held to within 1 percent for the first three modes by using at least 21 discrete masses in the solution.

Consideration of a uniform beam suggests that when employing trapezoidal integration in the influence coefficient calculations at least 50 integration intervals should be used. Extending the number of integration intervals to 200 or more will virtually remove all significant integration errors.

The method provides a means for the treatment of flexibilities such as those associated with joints. Frequently the contribution of joints to the flexibility of the system is a significant factor in the determination of the modal data.

In addition to mode deflections and frequencies, procedures are outlined for obtaining the slopes of the mode shapes and the moments associated with the modes.

The method is illustrated by applications to both a uniform beam and a typical research launch vehicle.

Langley Research Center,
National Aeronautics and Space Administration,
Langley Air Force Base, Va., February 16, 1962.

REFERENCES

1. Scanlan, Robert H., and Rosenbaum, Robert: Introduction to the Study of Aircraft Vibration and Flutter. The Macmillan Co., 1951, pp. 177-180.

2. Frazer, R. A., Duncan, W. J., and Collar, A. R.: Elementary Matrices and Some Applications to Dynamics and Differential Equations. Cambridge Univ. Press, 1952.

3. Michal, Aristotle D.: Matrix and Tensor Calculus. John Wiley & Sons, 1947.

4. Houbolt, John C., and Anderson, Roger A.: Calculation of Uncoupled Modes and Frequencies in Bending or Torsion of Nonuniform Beams. NACA TN 1522, 1948.

TABLE I.- FLEXURAL STIFFNESS DISTRIBUTION OF A LAUNCH VEHICLE

j	x_j, in.	EI, lb-in.^{2}	j	x_j, in.	EI, lb-in.^{2}	j	x_j, in.	EI, lb-in.^{2}
0	[a]0	1.485×10^9	53	174.86	10.11×10^9	105	355.08	4.670×10^9
1	4.01	1.485	54	175.66	3.780	106	356.08	9.000
2	4.51	1.485	55	180.19	3.591	107	356.08	9.000
3	4.58	1.500	56	184.68	2.503	108	360.78	4.12
4	6.51	2.420	57	185.18	3.384	109	365.47	4.51
5	7.01	8.580	58	[a]187.61	3.384	110	366.37	4.90
6	7.51	8.580	59	192.23	3.384	111	366.98	13.10
7	7.51	11.71	60	192.33	3.384	112	367.27	19.07
8	9.51	8.870	61	193.53	4.066	113	367.77	21.4
9	10.51	6.785	62	194.09	6.990	114	368.27	9.95
10	11.71	4.252	63	195.09	8.394	115	369.20	14.31
11	13.53	4.252	64	196.09	10.60	116	369.20	9.086
12	18.53	4.252	65	197.09	8.870	117	373.47	3.726
13	[a]23.53	4.252	66	198.09	6.276	118	[a]374.53	2.759
14	28.53	4.252	67	199.26	4.252	119	378.47	2.035
15	33.53	4.252	68	203.53	4.252	120	383.47	1.854
16	38.53	4.252	69	208.53	4.252	121	387.22	1.172
17	43.53	4.252	70	[a]212.53	4.252	122	387.22	.787
18	48.53	4.252	71	218.53	4.252	123	387.72	1.637
19	[a]53.53	4.252	72	223.53	4.252	124	387.72	2.229
20	58.53	4.252	73	228.53	4.252	125	388.48	5.713
21	63.53	4.252	74	[a]234.53	4.252	126	388.48	4.486
22	68.53	4.252	75	238.53	4.252	127	393.53	1.2
23	73.53	4.252	76	243.53	4.252	128	[a]396.53	1.2
24	78.53	4.252	77	248.53	4.252	129	398.53	1.2
25	[a]83.53	4.252	78	253.53	4.252	130	403.53	1.2
26	88.53	4.252	79	[a]256.53	4.252	131	408.53	1.2
27	93.53	4.252	80	258.53	4.252	132	413.53	1.2
28	98.53	4.252	81	263.53	4.252	133	[a]418.53	1.2
29	103.53	4.252	82	268.53	4.252	134	423.53	1.2
30	108.53	4.252	83	273.53	4.252	135	428.53	1.2
31	[a]113.53	4.252	84	278.53	4.252	136	433.53	1.2
32	118.53	4.252	85	[a]284.53	4.252	137	438.53	1.2
33	123.53	4.252	86	288.53	4.252	138	[a]443.53	1.2
34	128.53	4.252	87	293.53	4.252	139	448.53	1.2
35	133.53	4.252	88	298.53	4.252	140	453.53	1.2
36	138.53	4.252	89	303.53	4.252	141	458.53	1.2
37	[a]143.53	4.252	90	[a]308.53	4.252	142	[a]464.53	1.2
38	148.53	4.252	91	313.53	4.252	143	468.53	1.2
39	153.53	4.252	92	318.53	4.252	144	473.53	1.2
40	158.53	4.252	93	323.53	4.252	145	478.38	1.2
41	163.26	4.252	94	328.53	4.252	146	478.53	4.06
42	164.36	6.784	95	[a]330.53	4.252	147	479.03	1.18
43	165.36	8.871	96	333.53	4.252	148	[a]482.53	1.18
44	[a]165.53	9.638	97	338.53	4.252	149	485.98	1.18
45	166.36	11.71	98	343.53	4.252	150	489.98	1.40
46	167.48	9.913	99	348.53	4.252	151	490.48	.076
47	167.86	6.318	100	350.86	4.252	152	490.88	.076
48	170.26	2.678	101	352.06	6.804	153	495.98	2.39
49	172.86	4.894	102	353.06	8.871	154	496.48	.076
50	173.66	9.035	103	354.06	11.72	155	[a]499.53	.076
51	174.26	2.648	104	[a]354.53	8.276			
52	174.28	2.905						

[a]Locations of mass stations and limits of integration for equation (31).

TABLE II.- JOINT ROTATION CONSTANTS, κ_u

u	c_u, in.	κ_u, radians/in-lb
1	4.580	6.50×10^{-9}
2	167.48	4.00
3	174.28	20.00
4	192.30	6.50
5	355.08	4.00
6	366.98	3.00
7	388.48	20.00
8	478.38	20.00
9	490.88	20.00

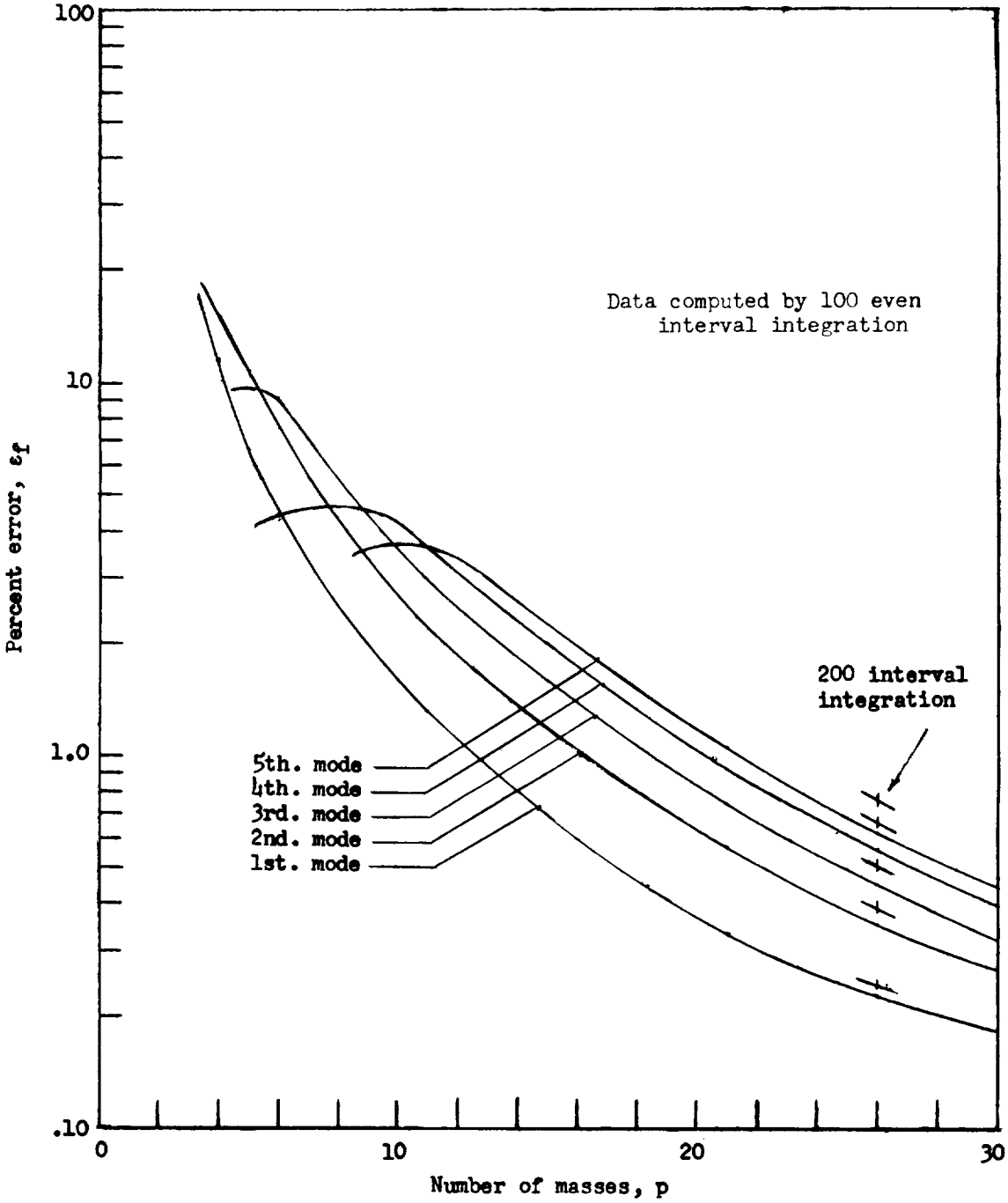

Figure 1.- Percent error in natural frequency of a uniform free-free beam as a function of the number of discrete masses used in the solution.

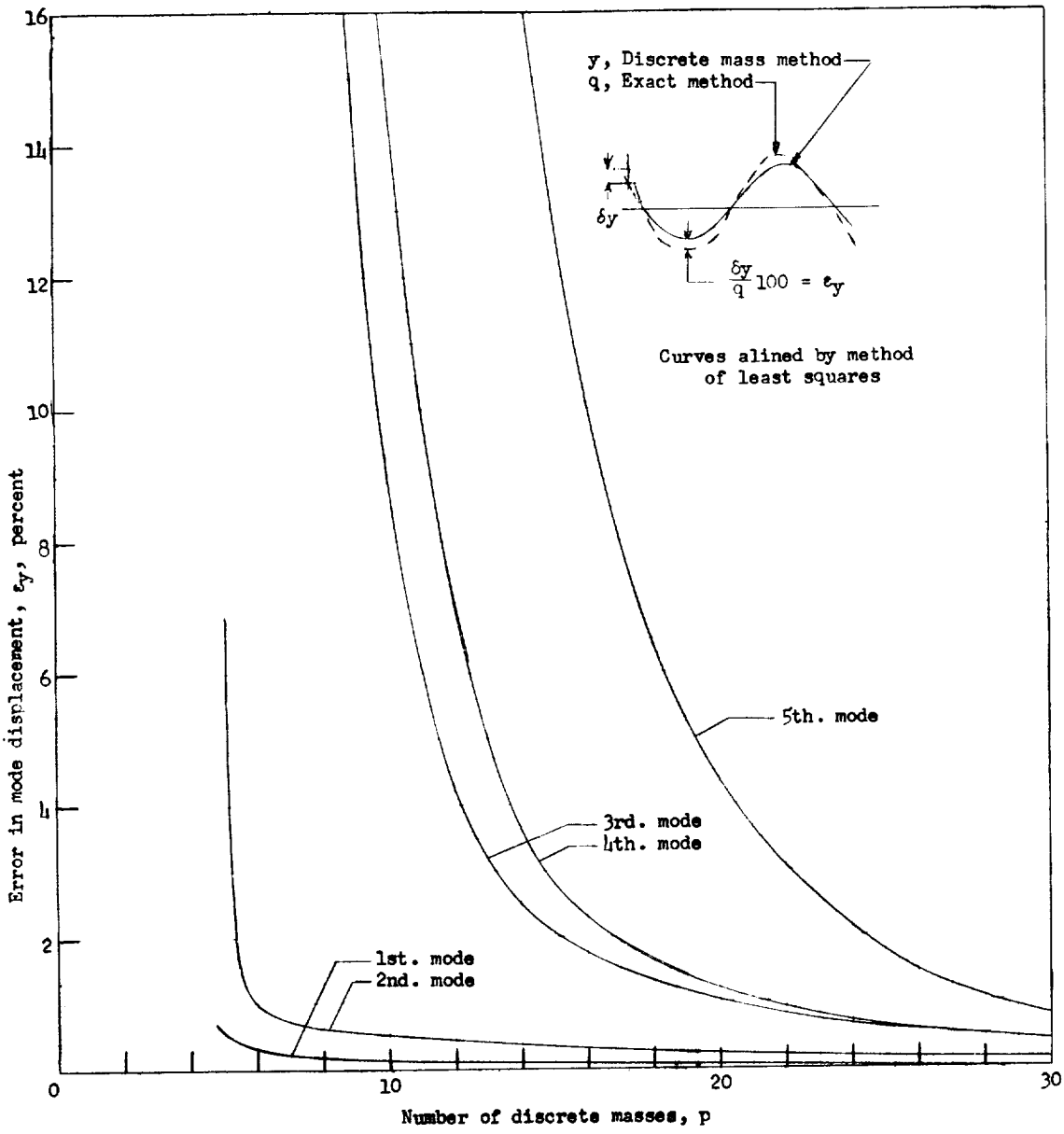

Figure 2.- Maximum error in the mode displacement of a uniform free-free beam as a function of the number of discrete masses used in the solution.

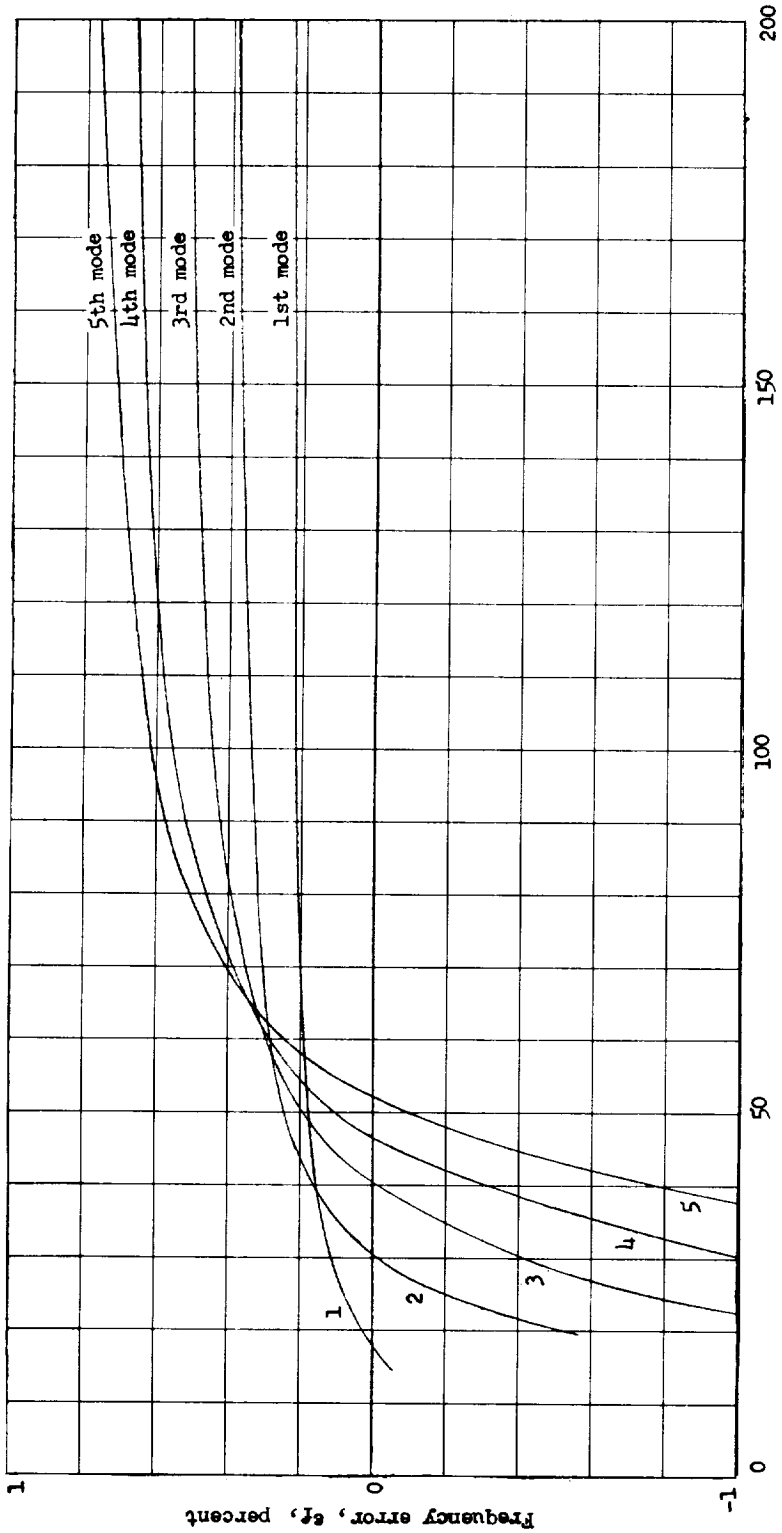

Figure 3.- Effects of the number of integration intervals on the frequency errors of a uniform beam represented by 26 discrete masses.

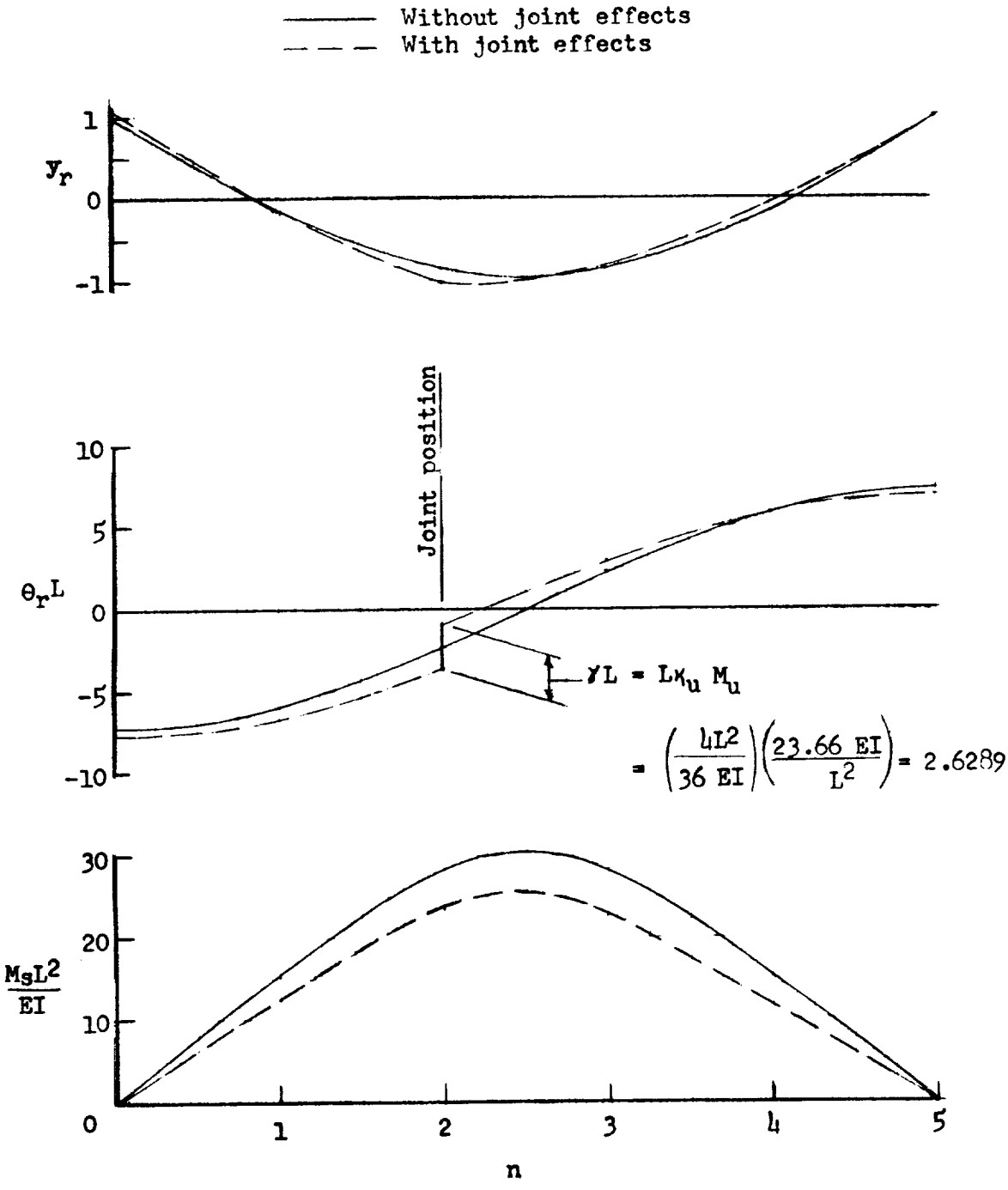

Figure 4.- Mode shapes, mode slopes, and mode moments for a uniform beam represented by 6 discrete masses.

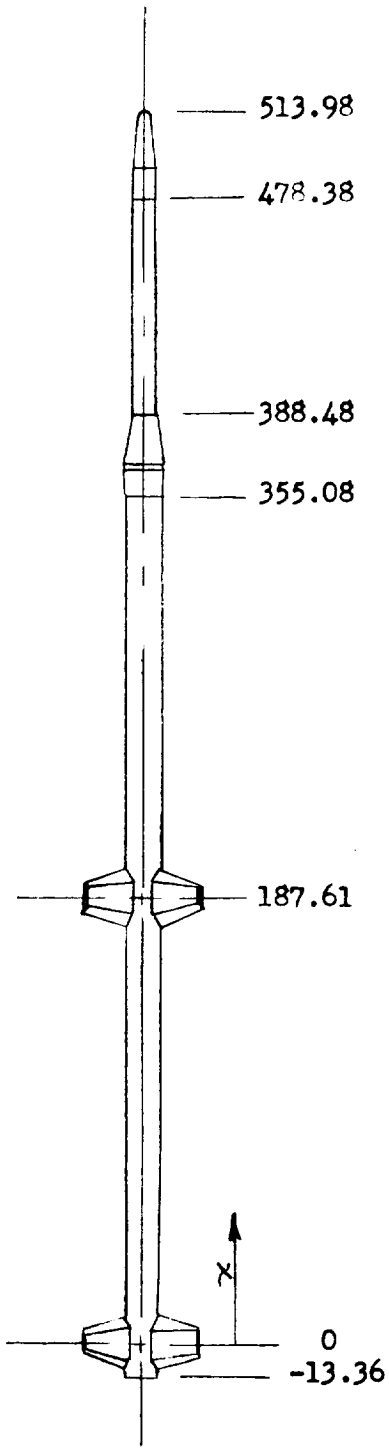

r	j	x_j (in.)	Mass (lb-sec^2/in.)
21	155	499.53	.076166
20	148	482.53	.13705
19	142	464.53	.20725
18	138	443.53	.24306
17	133	418.53	.20518
16	128	396.53	.21632
15	118	374.53	.13547
14	104	354.53	.40405
13	95	330.53	.73135
12	90	308.53	.39005
11	85	284.53	.78010
10	79	256.53	.53632
9	74	234.53	.56070
8	70	212.53	.56070
7	58	187.61	.82484
6	44	165.53	.38428
5	37	143.53	.73135
4	31	113.53	.73135
3	25	83.53	.73135
2	19	53.53	.73135
1	13	23.53	.75304
0	0	0	.64974

Figure 5.- Discrete mass representation of a typical three-stage space vehicle.

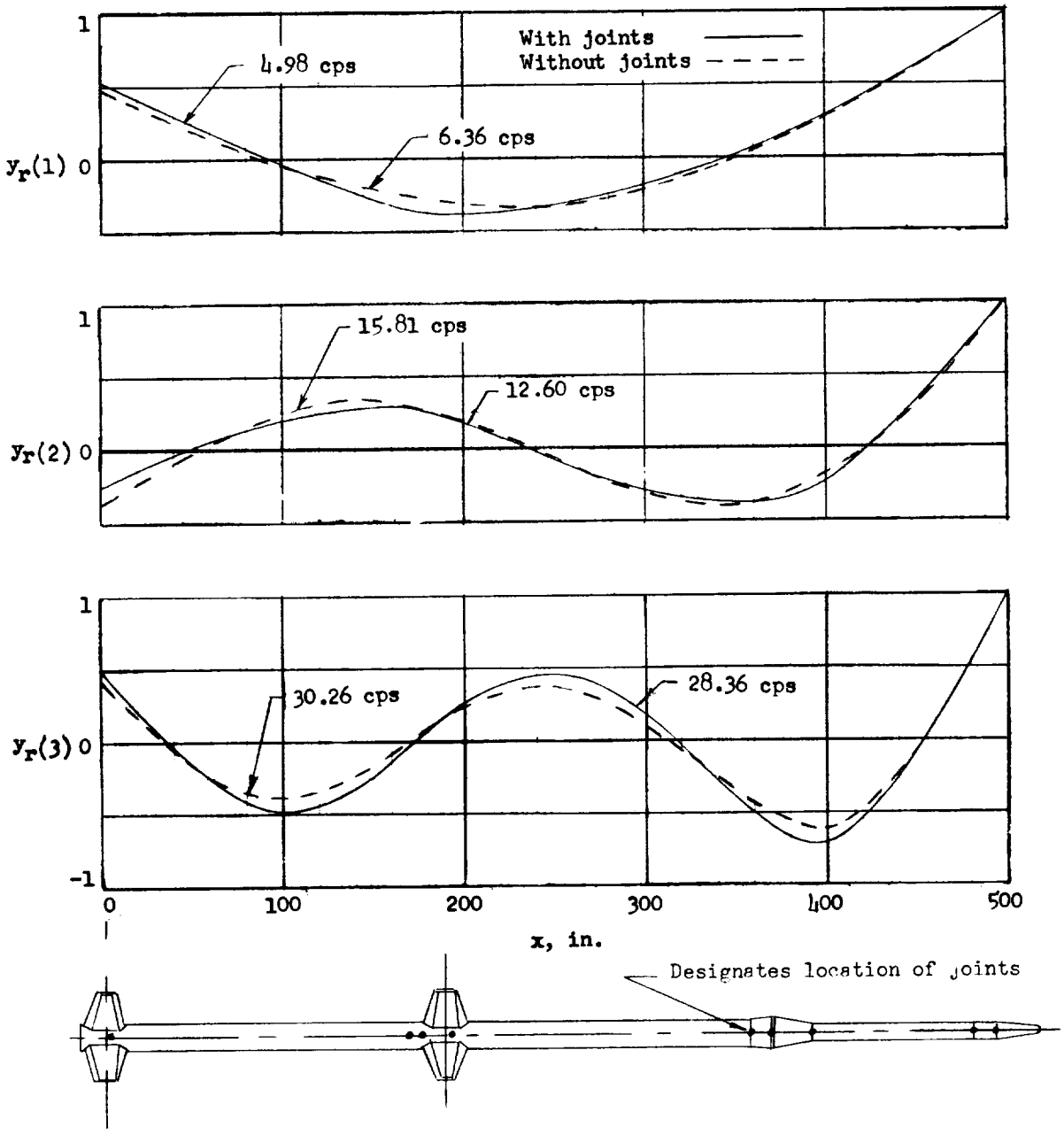

Figure 6.- Natural frequencies and mode shapes for the first three natural modes of a three-stage launch vehicle.

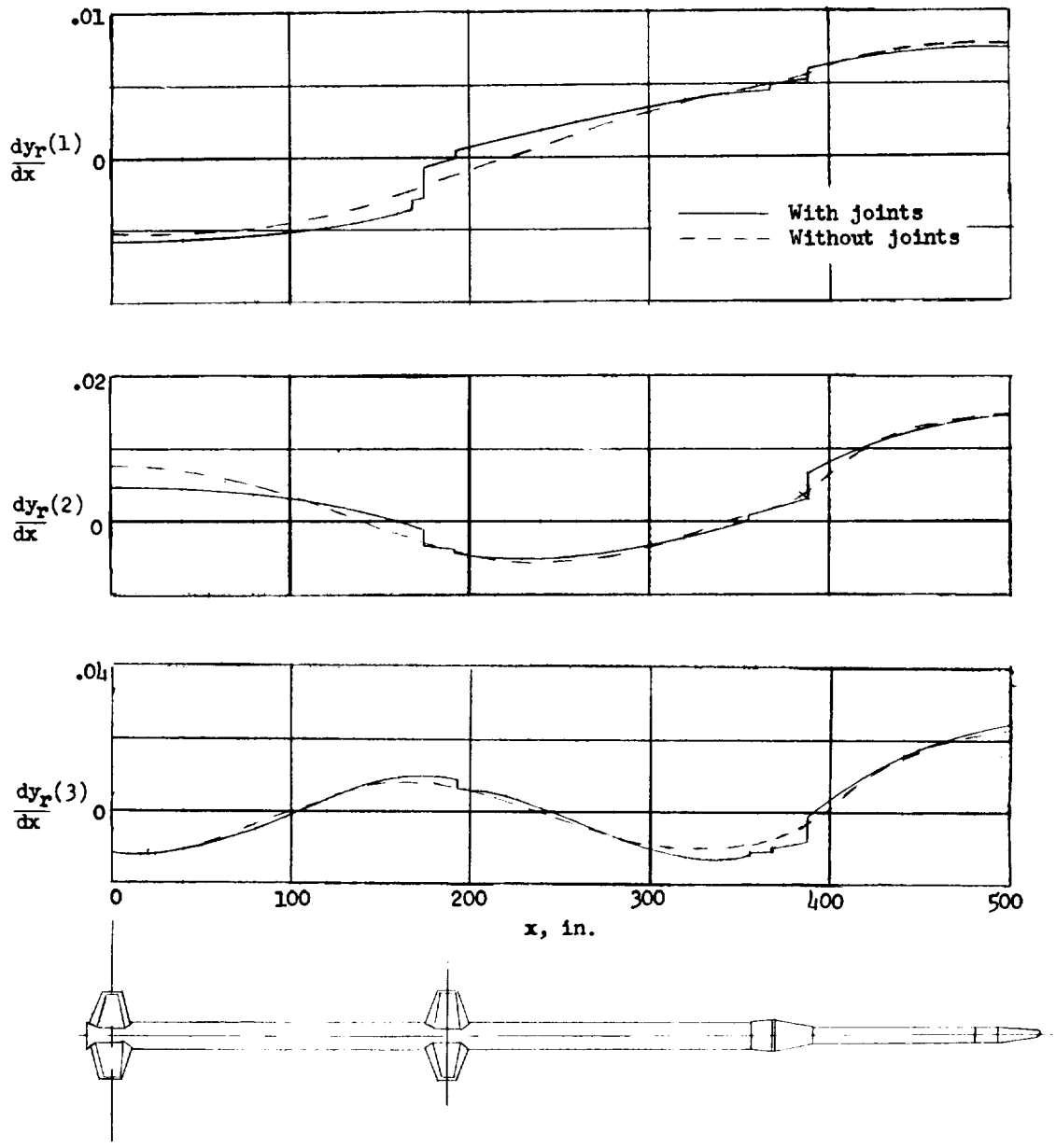

Figure 7.- Mode slopes for the first three natural modes of a three-stage launch vehicle.

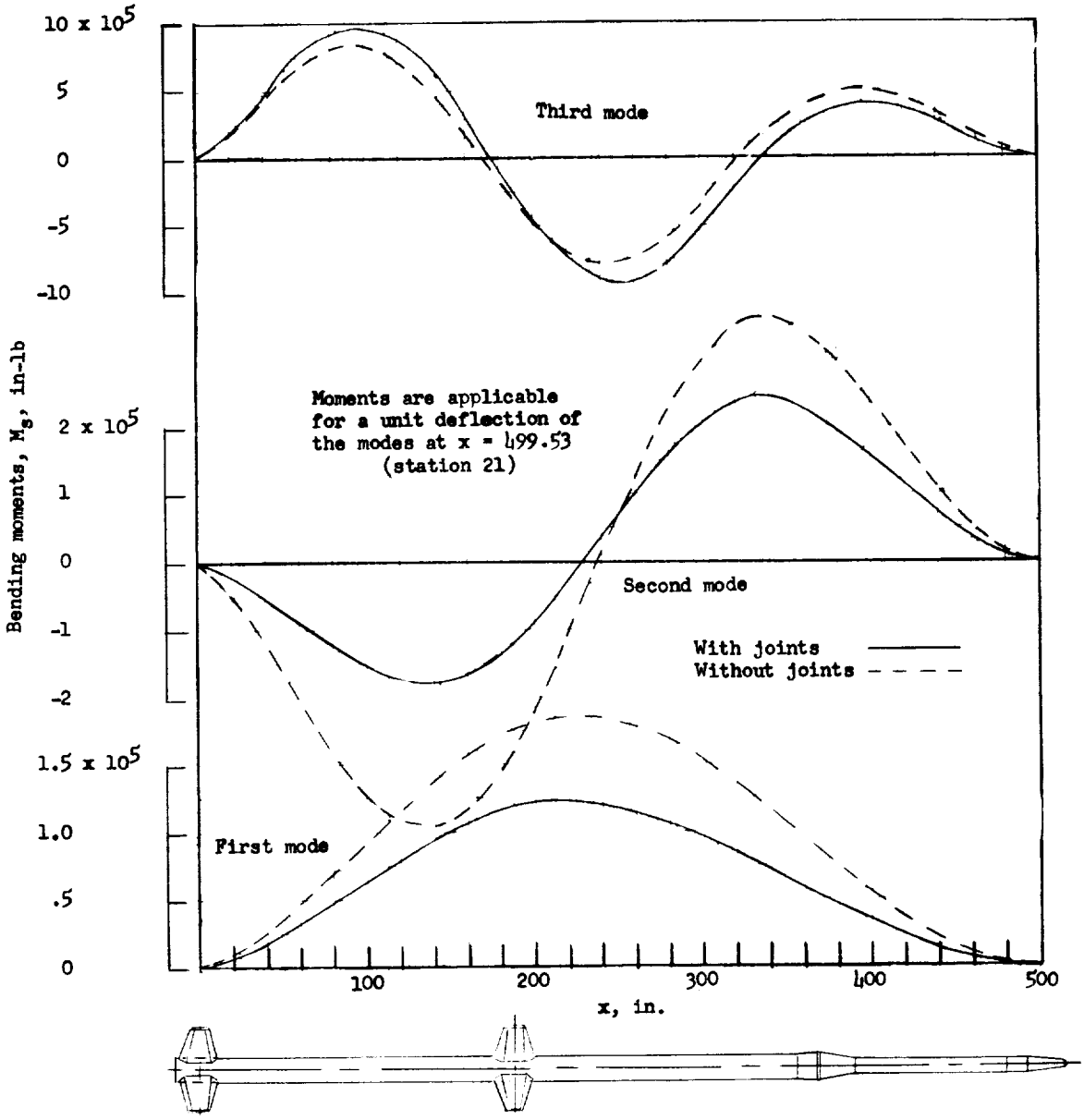

Figure 8.- Moment curves for the first three natural modes of a three-stage launch vehicle.

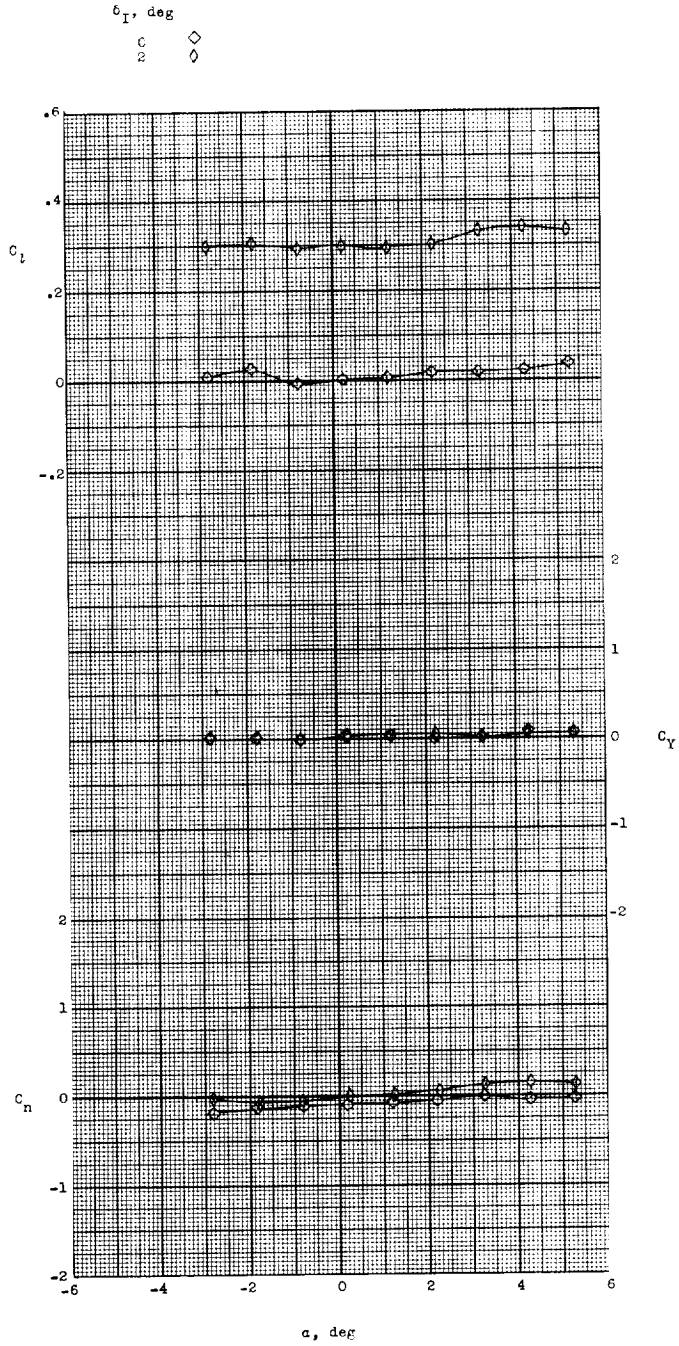

(c) M = 2.36; β = 0°.

Figure 17.- Continued.

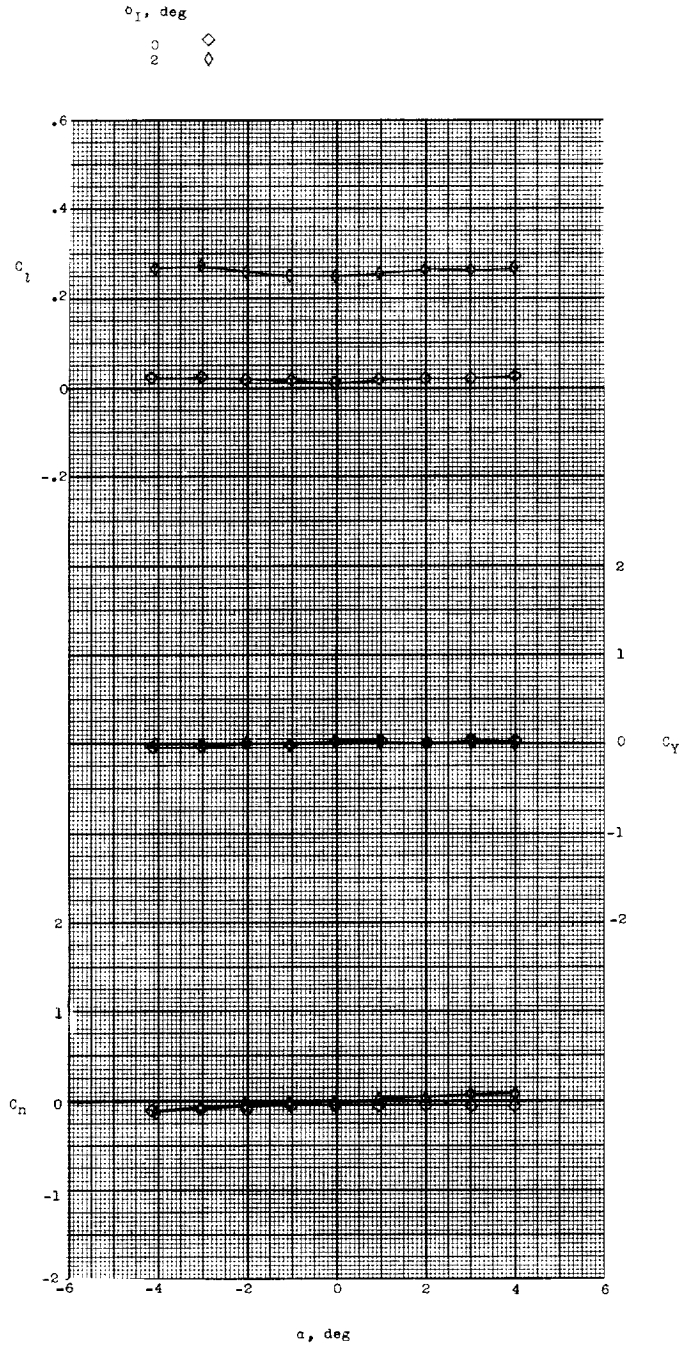

(d) M = 2.86; $\beta = 0^o$.

Figure 17.- Continued.

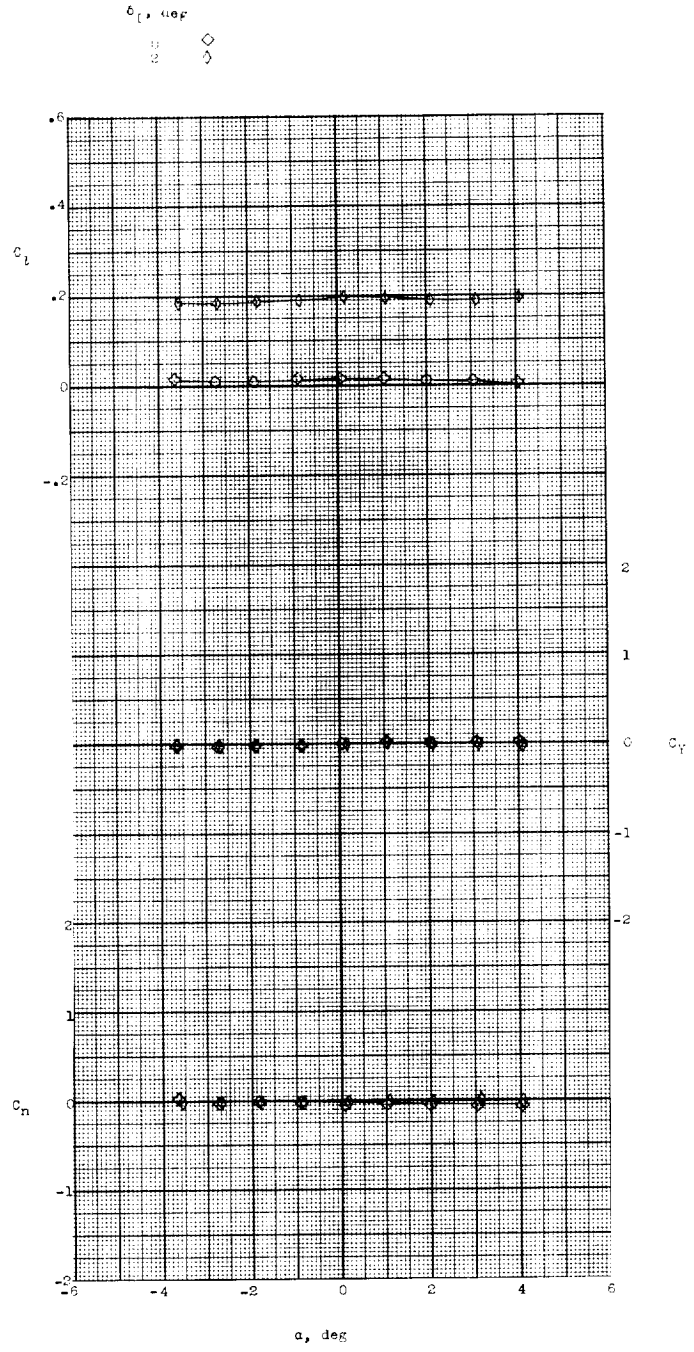

(e) M = 3.96; β = 0°.

Figure 17.- Continued.

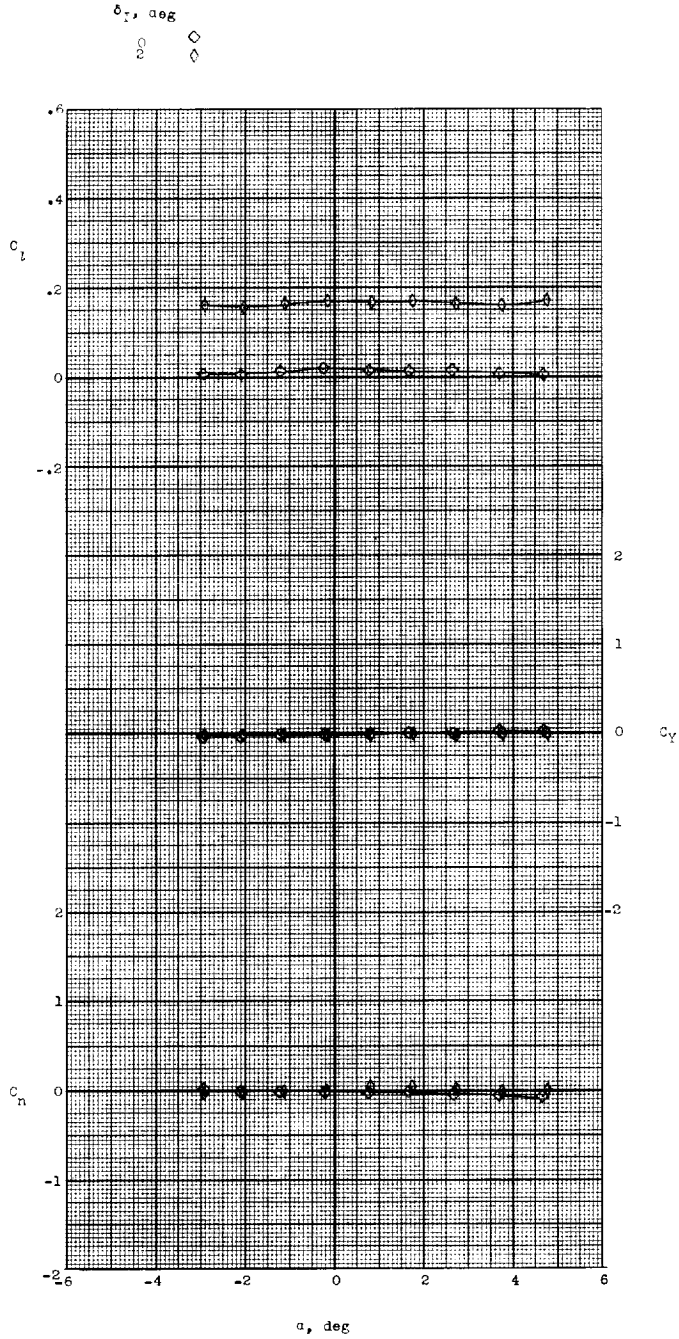

(f) M = 4.63; β = 0°.

Figure 17.- Concluded.

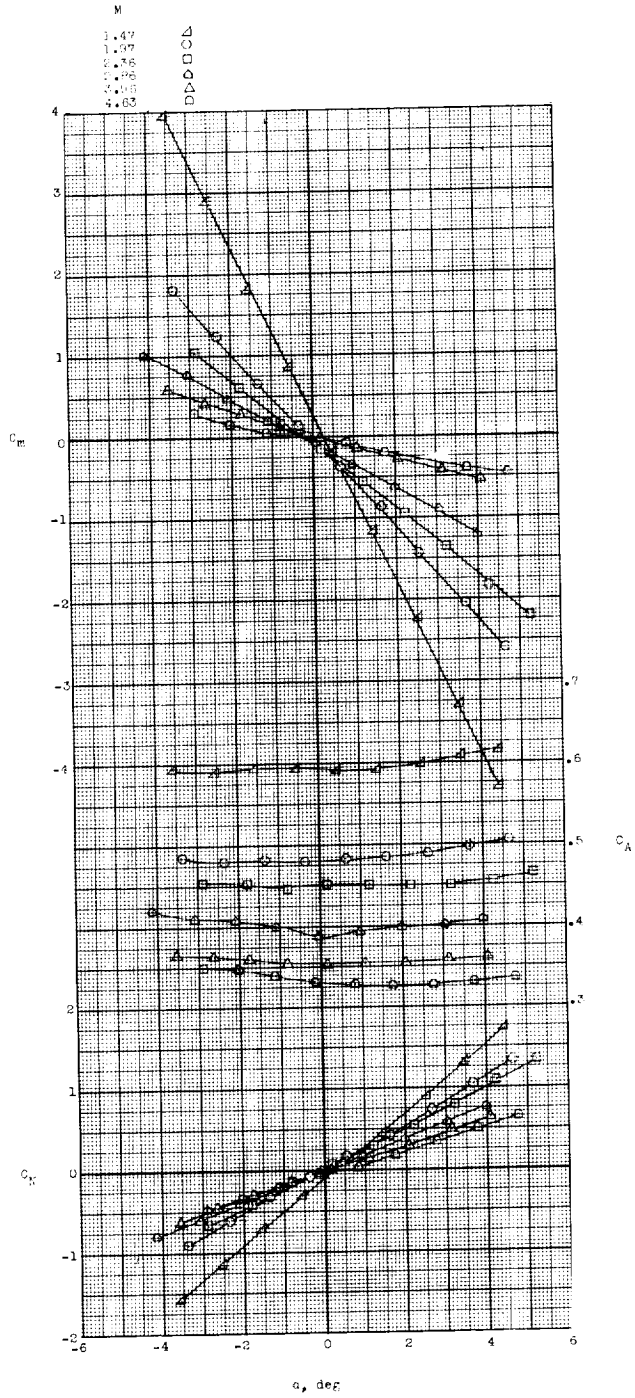

Figure 18.- Variation of pitch characteristics with angle of attack at six Mach numbers for two-stage configuration without auxiliary rocket motors. 12-sq-ft, A = 1.5 fins; $\delta_I = 0^o$; $\beta = 0^o$.

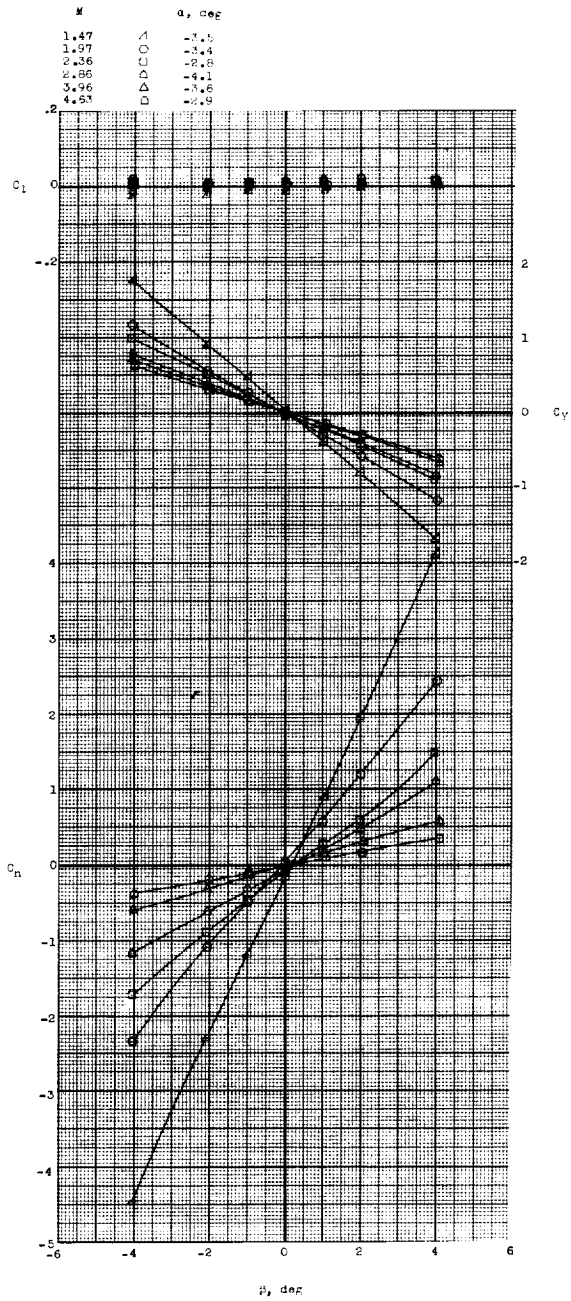

(a) $\delta_I = 0^\circ$; $\alpha \approx -4^\circ$.

Figure 19.- Variation of lateral characteristics with angle of sideslip at six Mach numbers for two-stage configuration without auxiliary rocket motors. 12-sq-ft, A = 1.5 fins.

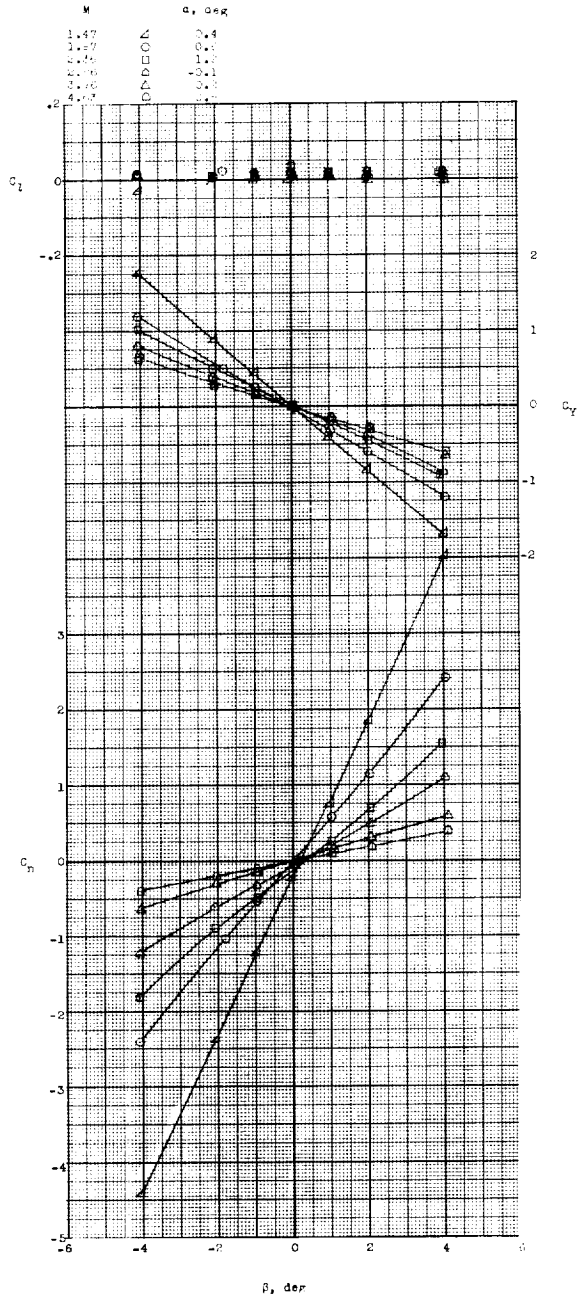

(b) $\delta_I = 0^\circ$; $\alpha \approx 0^\circ$.

Figure 19.- Continued.

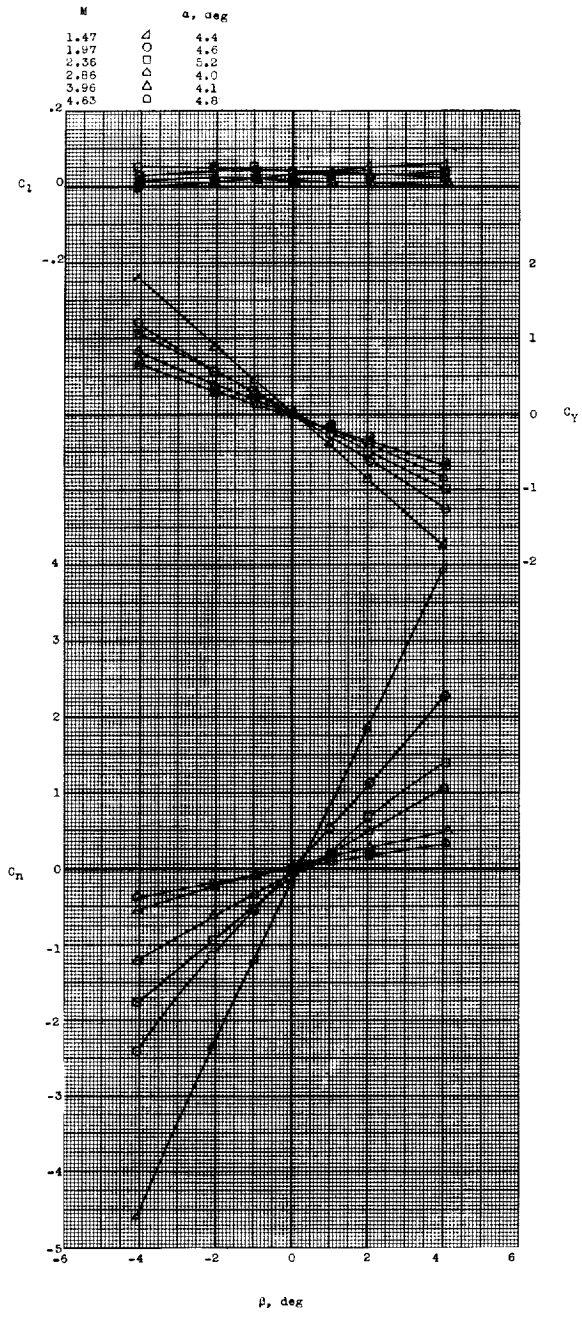

(c) $\delta_I = 0^\circ$; $\alpha \approx 4^\circ$.

Figure 19.- Concluded.

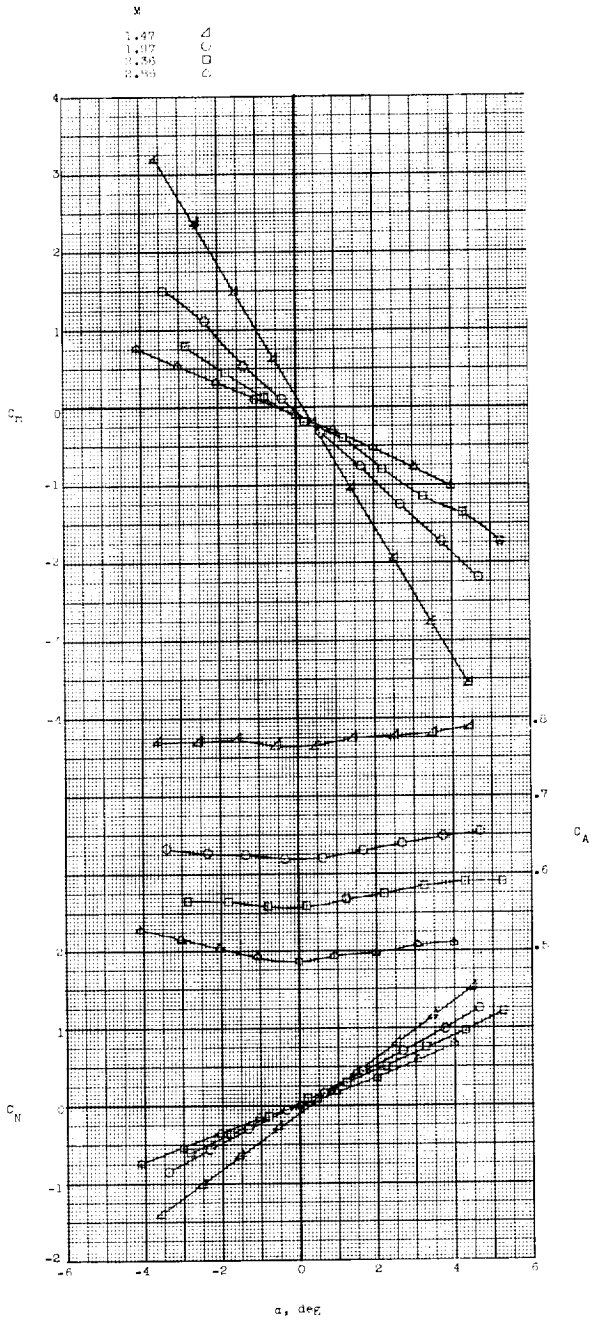

(a) $\delta_I = 0^\circ$; $\beta = 0^\circ$.

Figure 20.- Variation of pitch characteristics with angle of attack at four Mach numbers for two-stage configuration. 10-sq-ft, A = 1.5 fins.

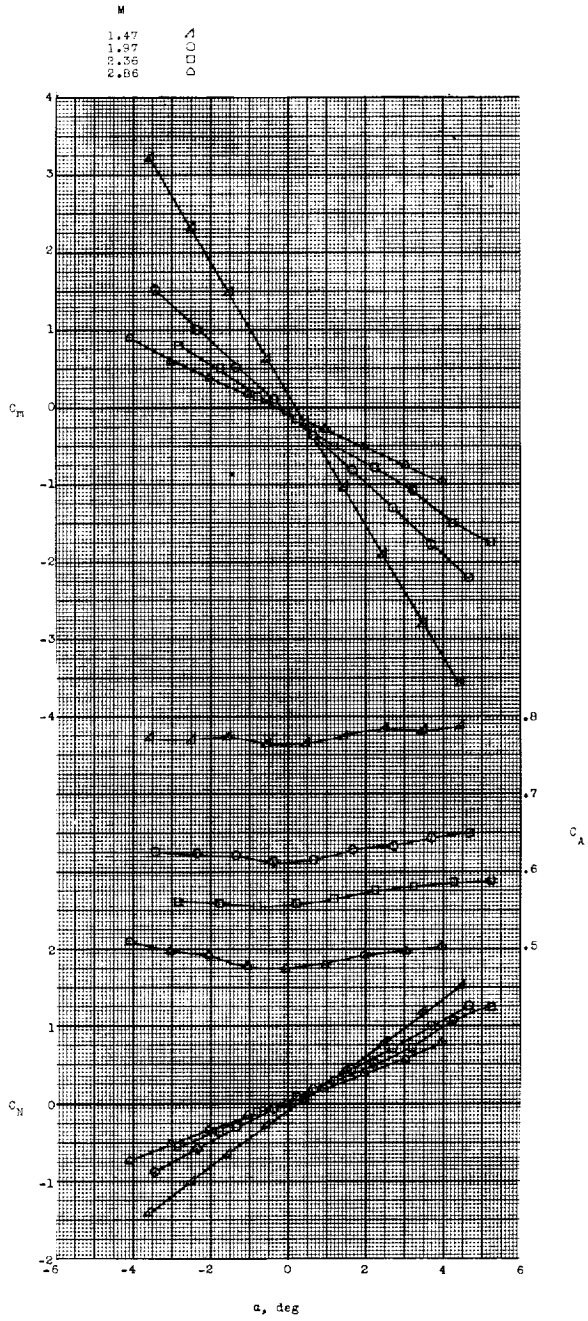

(b) $\delta_I = 2^o$; $\beta = 0^o$.

Figure 20.- Concluded.

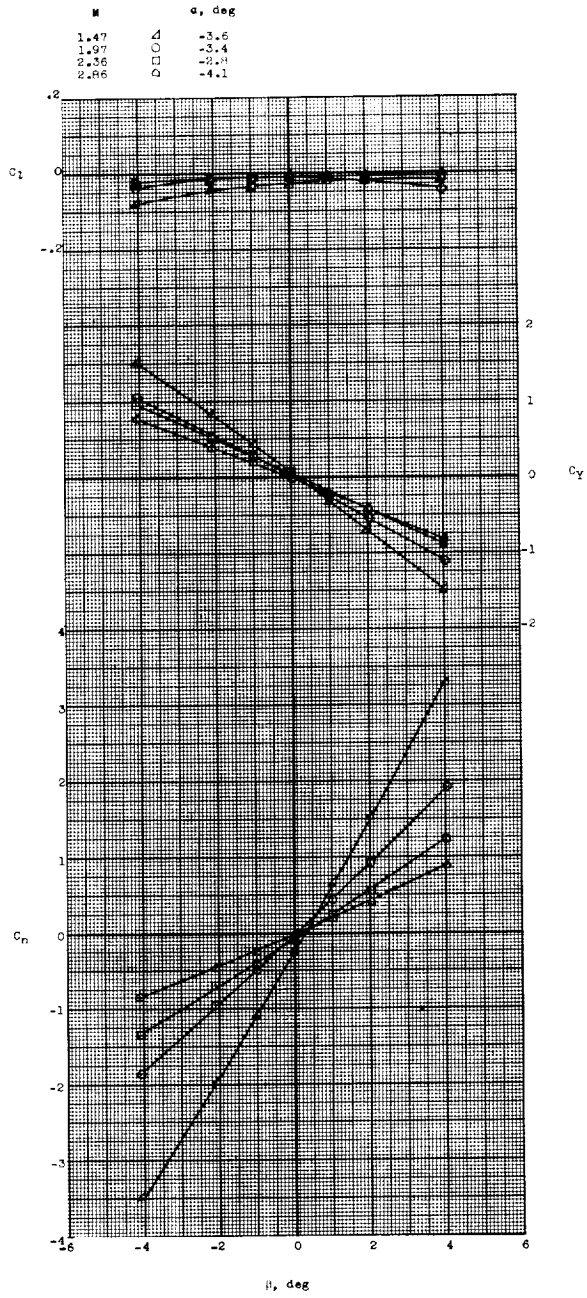

(a) $\delta_I = 0^\circ$; $\alpha \approx -4^\circ$.

Figure 21.- Variation of lateral characteristics with angle of sideslip at four Mach numbers for two-stage configuration. 10-sq-ft, A = 1.5 fins.

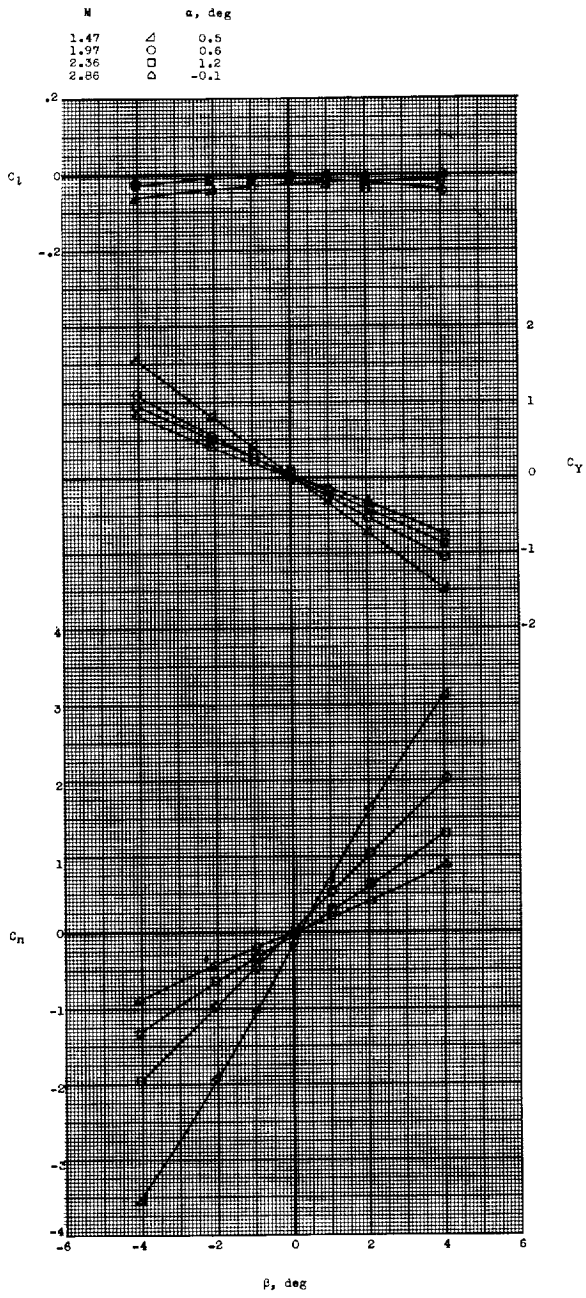

(b) $\delta_I = 0^\circ$; $\alpha \approx 0^\circ$.

Figure 21.- Continued.

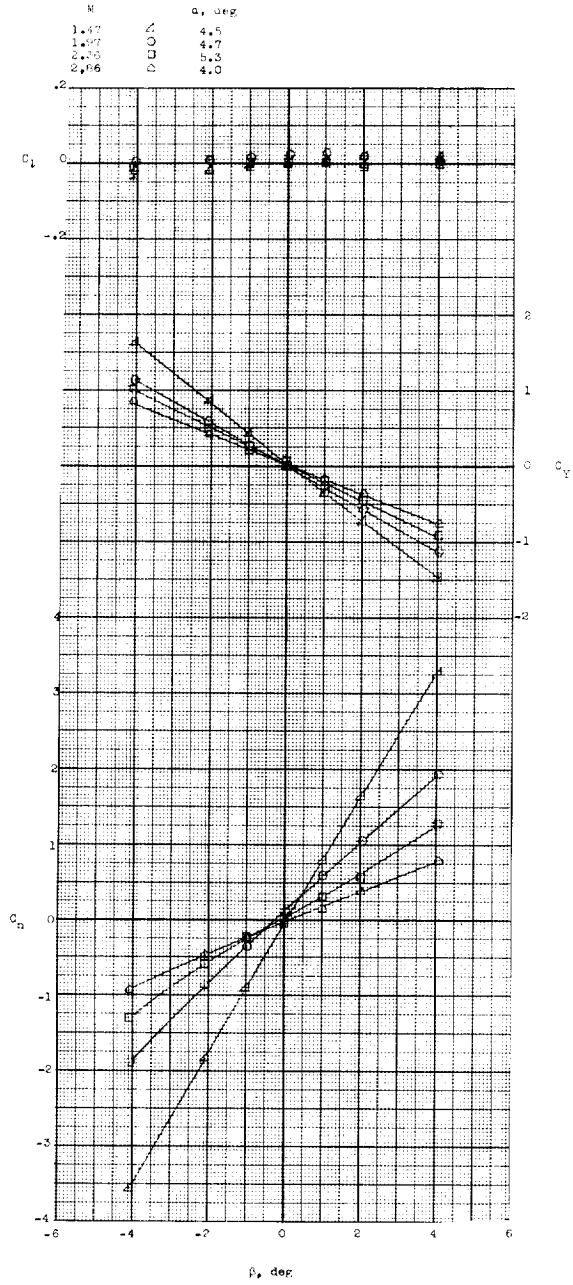

(c) $\delta_I = 0^\circ$; $\alpha \approx 4^\circ$.

Figure 21.- Concluded.

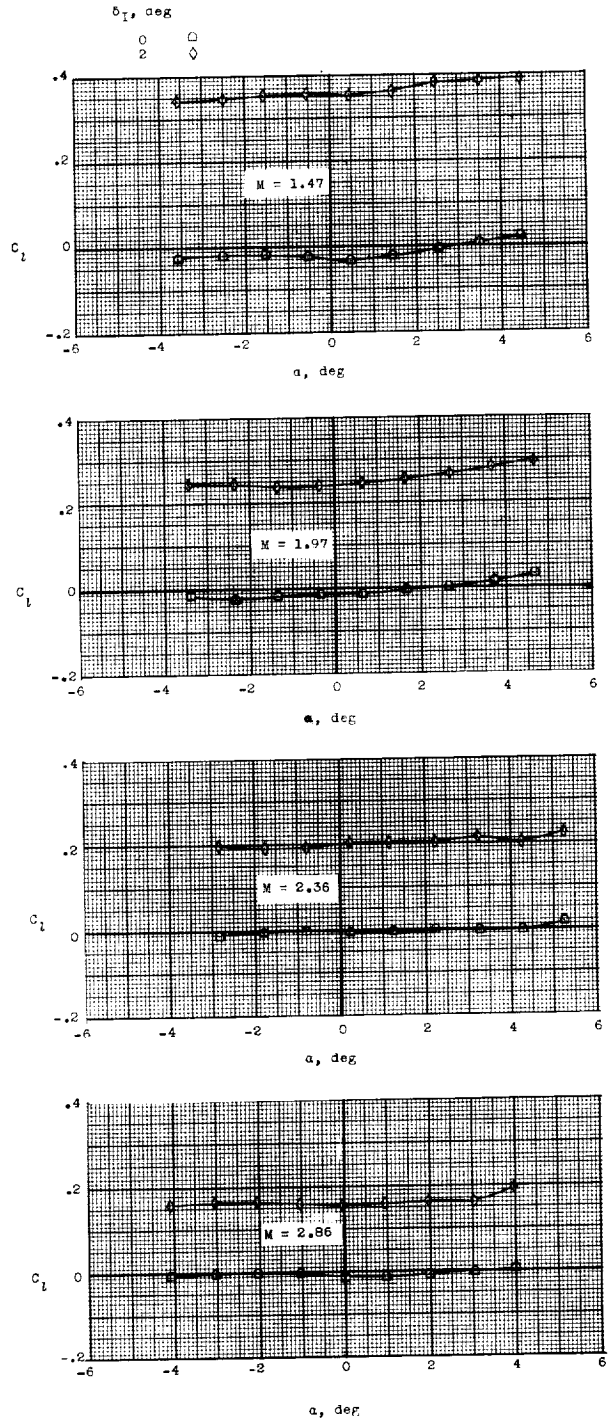

Figure 22.- Variation of rolling moment with angle of attack for two-stage configuration with fin cant. 10-sq-ft, A = 1.5 fins.

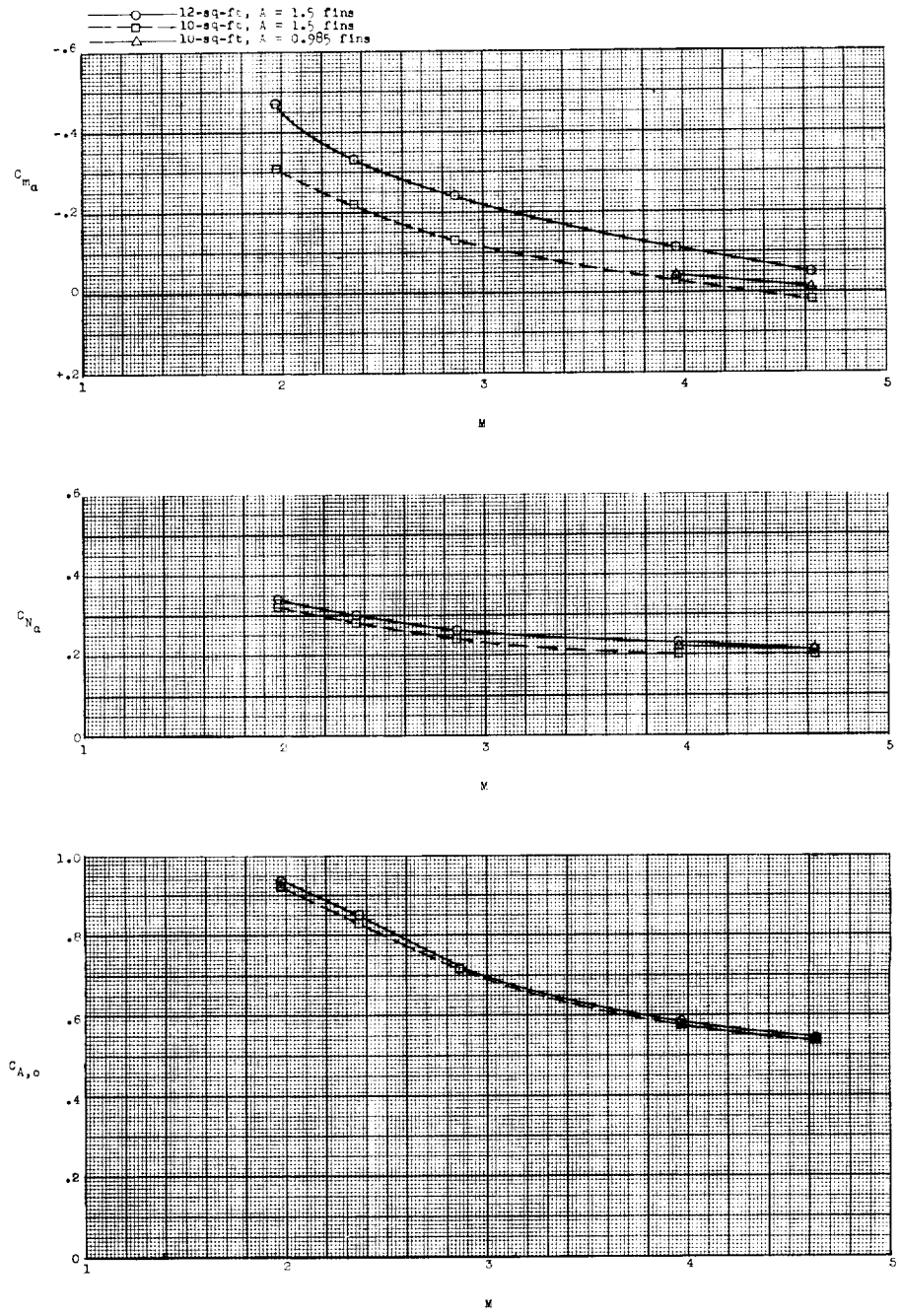

Figure 23.- Variation of pitching-moment derivative C_{m_α}, normal-force derivative C_{N_α}, and axial-force coefficient $C_{A,o}$ with Mach number for three-stage configurations.

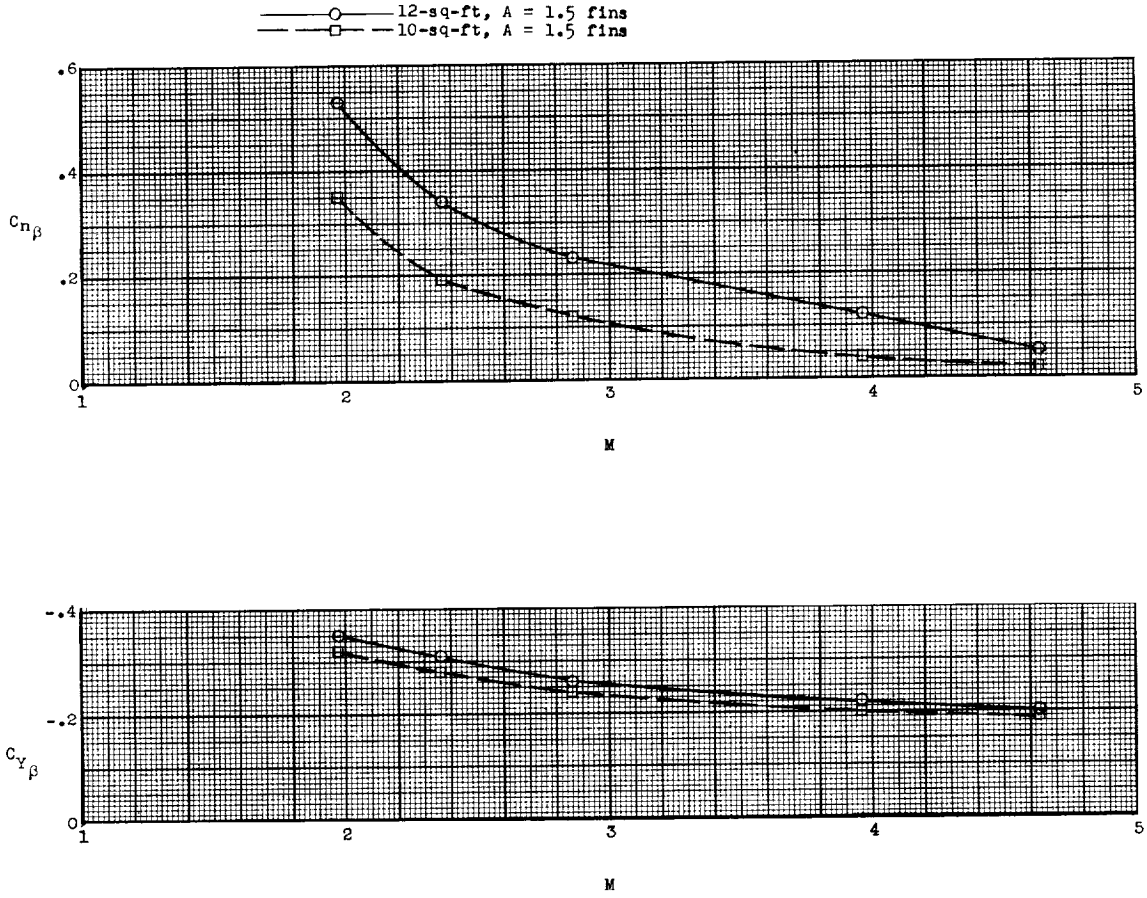

Figure 24.- Variation of yawing-moment derivative C_{n_β} and side-force derivative C_{Y_β} with Mach number for three-stage configurations.

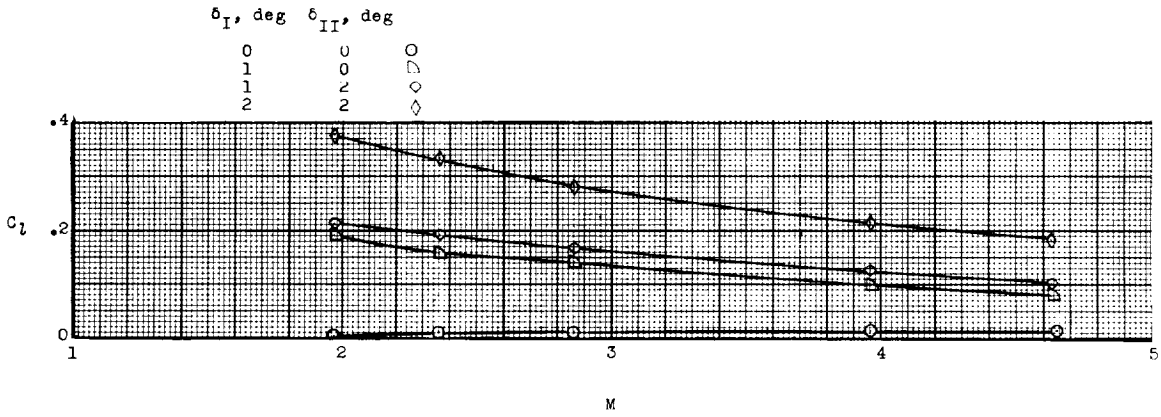

(a) 12-sq-ft, A = 1.5 fins.

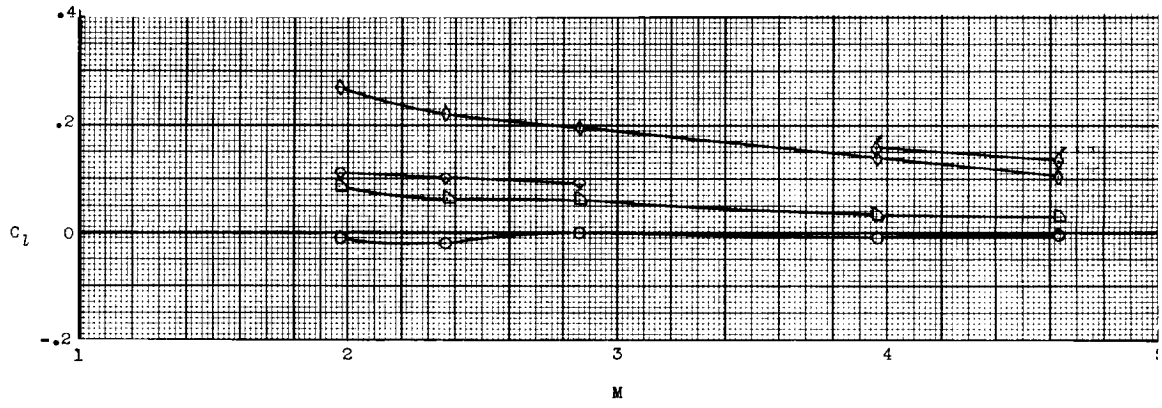

(b) 10-sq-ft, A = 1.5 fins. (Flagged symbols denote 10-sq-ft, A = 0.985 fins.)

Figure 25.- Variation of rolling-moment coefficient C_l with Mach number for three-stage configurations.

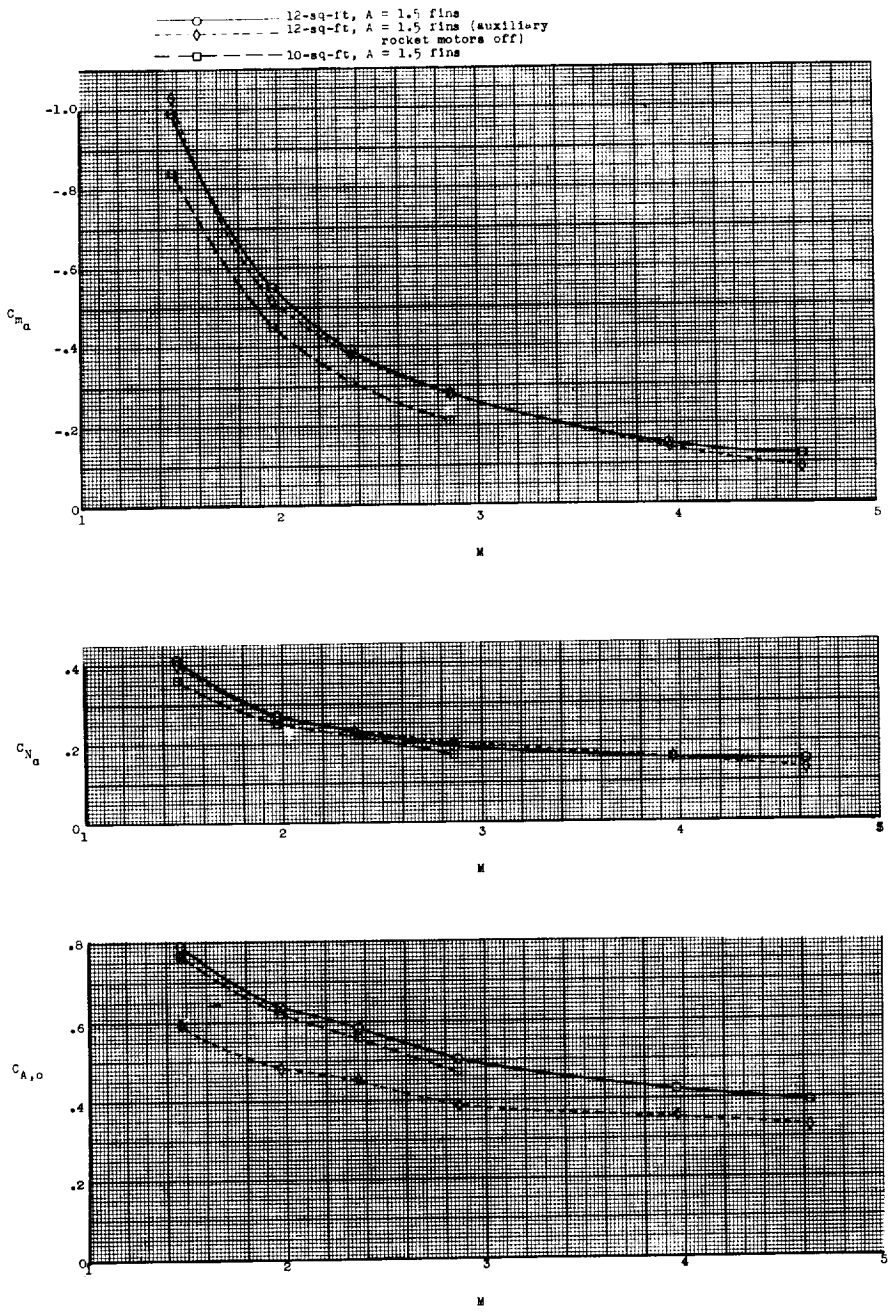

Figure 26.- Variation of pitching-moment derivative C_{m_α}, normal-force derivative C_{N_α}, and axial-force coefficient $C_{A,o}$ with Mach number for two-stage configurations.

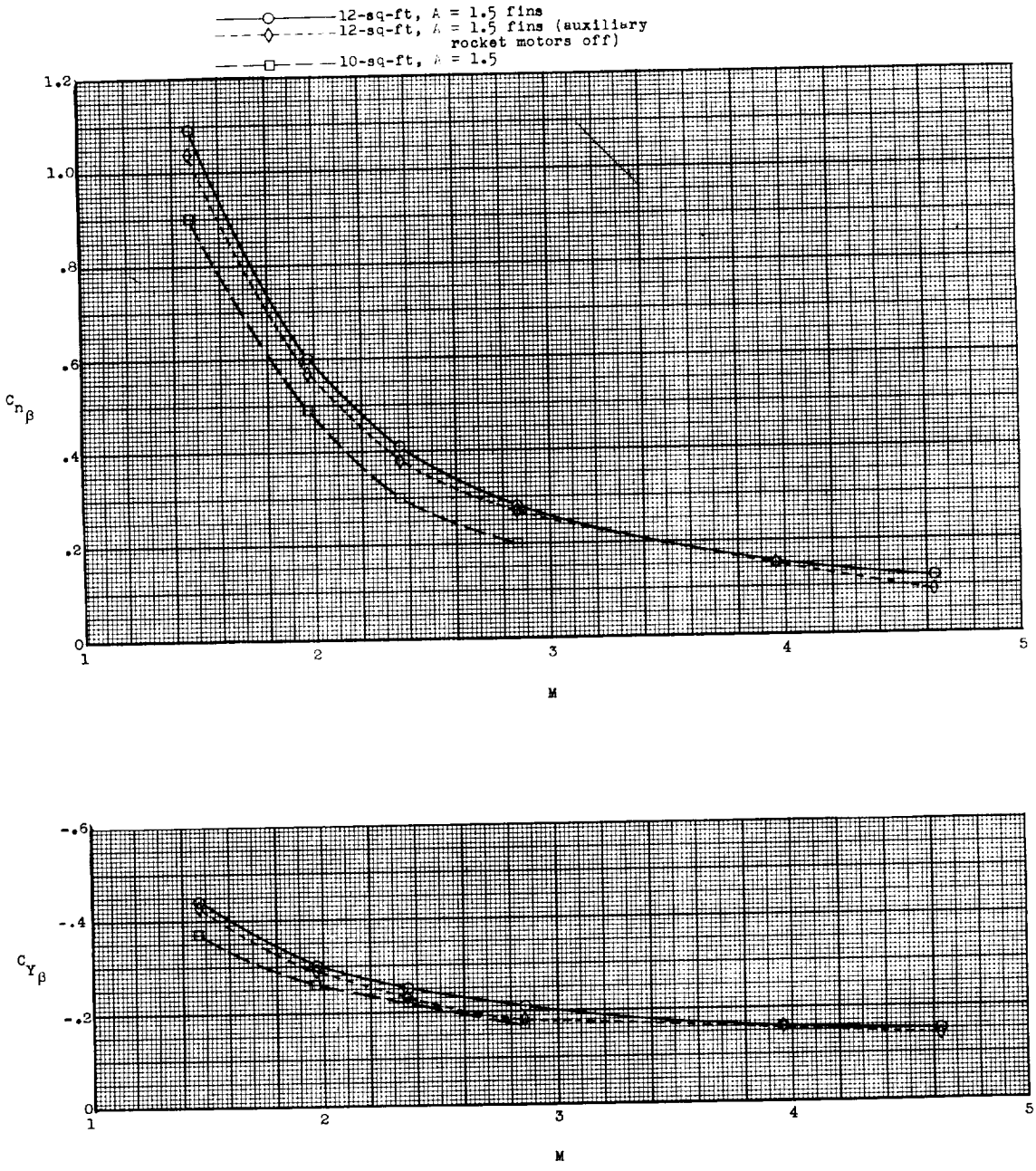

Figure 27.- Variation of yawing-moment derivative C_{n_β} and side-force derivative C_{Y_β} with Mach number for two-stage configurations.

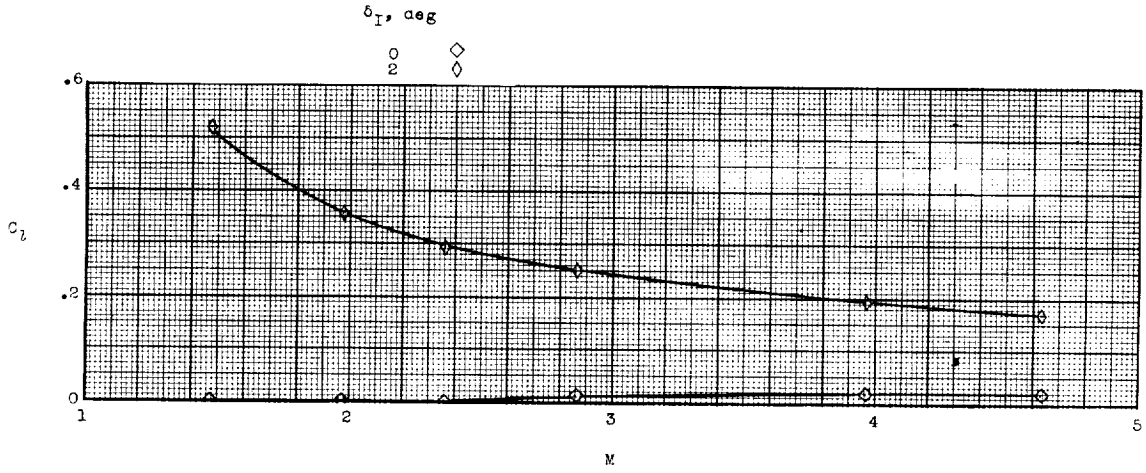

(a) 12-sq-ft, A = 1.5 fins.

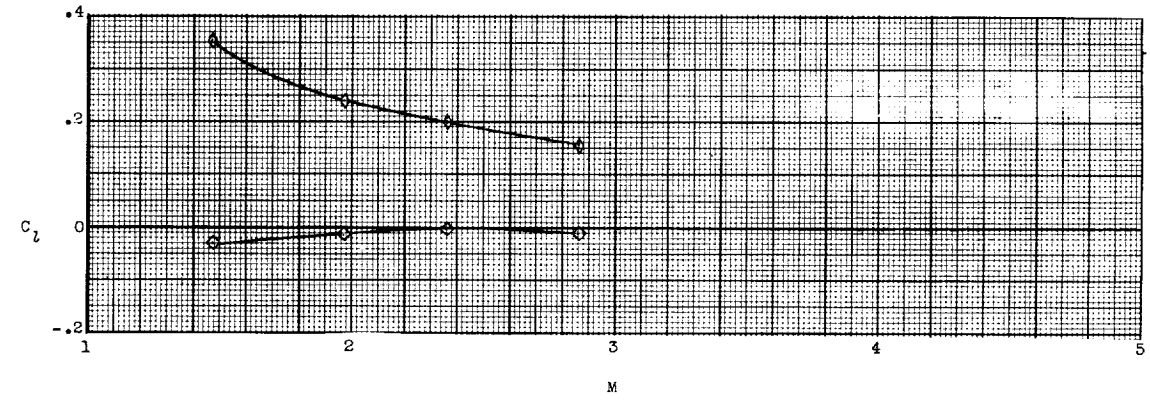

(b) 10-sq-ft, A = 1.5 fins.

Figure 28.- Variation of rolling-moment coefficient C_l with Mach number for two-stage configurations.

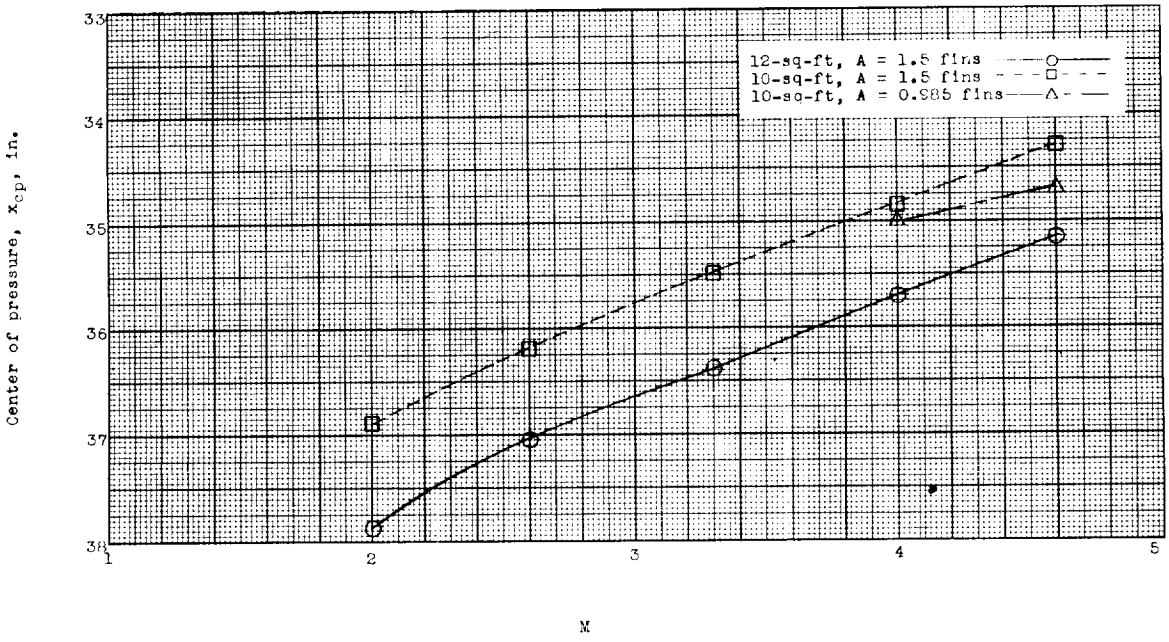

(a) Three-stage configuration.

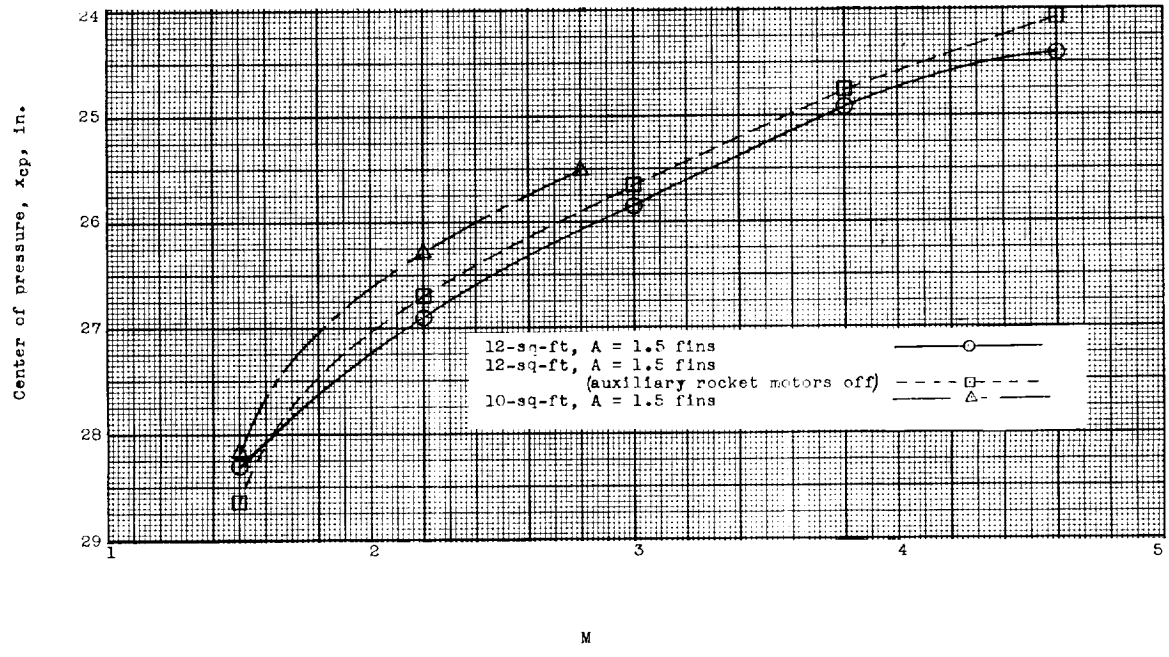

(b) Two-stage configuration.

Figure 29.- Variation of center-of-pressure location with Mach number for all configurations tested.